New Mapping Schemes for Multi-dimensional Constellation in MIMO-BICM-ID Systems

Ali Reza Rabbani Abolfazli

A thesis

in

The Department

of

Electrical and Computer Engineering

Presented in Partial Fulfillment of the Requirements

for the Degree of Master of Applied Science (Electrical Enginnering) at

Concordia University

Montreal, Quebec, Canada

April 2007

Your file Votre référence
ISBN: 978-0-494-28924-2
Our file Notre référence
ISBN: 978-0-494-28924-2

Abstract

New Mapping Schemes for Multi-dimensional Constellation
in MIMO-BICM-ID Systems

Ali Reza Rabbani Abolfazli

Recently, Multiple Input and Multiple Output (MIMO) systems have shown a tremendous potential to increase the spectral efficiency and the reliability of wireless communication. These aspects are quantified in terms of the spatial multiplexing gain and the diversity gain respectively. It was shown that there is a trade-off between diversity and multiplexing gains. Bit Interlevead Coded Modulation with Iterative Decoding (BICM-ID) for Multiple Input and Multiple Output channels has recently been addressed as an effective mean to achieve high data rates while maintaining high diversity.

It has been shown that, when signal constellation, interleaver and error control code are fixed, signal mapping has a crucial influence on the error performance of a BICM-ID system. The role of signal mapping applies to the error performance of MIMO-BICM-ID system.

In this thesis, the design of constellation mapping for MIMO-BICM-ID system is studied. Based on minimizing pair-wise error probability, a design criterion is proposed to find the optimal constellation mapping for MIMO-BICM-ID. To reduce computational complexity of exhaustive search, Binary Switching Algorithm is improved to find the optimal solution. Using the design criterion and employing the Binary Switching Algorithm, some optimal constellation mappings are found for 2-dimensional and 3-dimensional cases.

A measurement based on mutual information is developed to evaluate the proposed constellation mappings. It is shown that proposed mappings sacrifice bit-wise mutual information without *a priori* information but improve significantly when perfect *a priori* knowledge is available. At the receiver, to avoid the computational complexity of the optimal Maximum-Likelihood (ML) detector, List Sphere Decoder (LSD) is used as the inner detector.

Simulation results demonstrate that proposed schemes outperform conventional ones significantly at high signal to noise ratio (SNR) over fading channels. System simulations are carried out specifically for 2-dimensional QPSK, 2-dimensional 8QAM and 3-dimensional QPSK constellations/mappings. Results show an improvement of 1.3 dB, 1.6 dB and 1.8 dB compared to conventional constellation mappings over slow fading channels, respectively. This improvement increase to 3.5 dB, 2.7 dB and 2.4 dB for fast fading channels.

Acknowledgements

I would like to express my deepest gratitude to my supervisor Dr. Yousef R. Shayan for his valuable guidance, advice, encouragements and financial supports. Without him, I could not pursue Master degree in Concordia University. Thank you Dr. Shayan for always believing in my capabilities.

I would like to express my appreciation to Dr. Xiaofeng Wang for his great ideas, helps, generously answering my questions and providing useful information regarding my thesis.

I owe special thanks to my parents for their helps, encouragements, emotional and financial supports. Also many thanks to my sisters for their encouragements and always being there for me. Last but not least, I wish to thank my beloved wife, Sanaz, for her endless love, continuous supports and encouragements. Thank you Sanaz for your patience, understanding and accepting to live far from each other for 2 years.

I indebted to my friend Dr. Zhiyuan Wu for his suggestions and proof reading of my thesis. I owe him for all Saturdays he sat for helping me.

I also extend my thanks to my defense committee and to the Faculty and staff of Electrical and Computer Engineering Department at Concordia University.

Finally, I wish to thank all my friends for their encouragements and supports.

To my parents and Sanaz

Contents

List of Tables

List of Figures

List of Acronyms

APP	a posteriori
AWGN	Additive White Gaussian Noise
BCJR	Bahl, Cocke, Jelinik and Raviv
BER	Bit Error Rate
BICM	Bit Interleaved Coded Modulation
BICM-ID	Bit Interleaved Coded Modulation with Iterative Decoding
BSA	Binary Switching Algorithm
CSI	Channel State Information
D-Blast	Diagonal Bell-labs Layered Space Time Architecture
ED	Euclidean Distance
HD	Hamming Distance
i.i.d	Independently Identically Distributed
LLR	Log-Likelihood Ratio
LSD	List Sphere Decoder
MAP	Maximum a posteriori
MIMO	Multiple Input Multiple Output
ML	Maximum Likelihood
PEP	Pairwise Error Probability
PSK	Phase Shift Keying
QAM	Quadrature Amplitude Modulation
QPSK	Quadrature Phase Shift Keying
SD	Sphere Decoder
SISO	Single Input Single Output
SISO	Soft Input Soft Output
SNR	Signal to Noise Ratio
TCM	Trellis Coded Modulation
TTCM	Turbo TCM

Chapter 1

Introduction

A general digital communication system consists of three basic sections: Transmitter, communication channel and receiver. The transmitter task is to convert information bits to signals that can be transmitted over the channel. The channel is the physical medium used to send signals from transmitter to receiver. The receiver is the end of a communication system which detects the information bits with lowest possible probability of error. Using error correction codes in a real-time communication system improves error performance at the cost of bandwidth.

Increasing demand for using wireless communication systems, expecting good quality of service and limitation in availability of radio spectrum, have shifted the researchers' focus towards designing more spectral efficient systems. In single antenna wireless communication systems, the Shannon capacity limit [1] can be achieved through advanced codes, such as Turbo codes [2] and low density parity check codes [3][4]. Utilizing multiple antennas at both transmitter and receiver sides is another technique which allows high data rates as well as reliable communication [5] [6].

1.1 Literature Survey

By increasing constellation points or using multilevel/phase modulation in coded schemes, a good coding gain without increasing bandwidth can be achieved. The integration of encoding and modulation yields to a digital coded modulation system which was studied first by Massey [7]. In 1982, Ungerboeck introduced a *Trellis-coded modulation* (TCM) system as a bandwidth-efficient signaling over an additive white Gaussian noise (AWGN) channel [8]. Ungerboeck proposed that for the systems using non-binary signal constellation, the primary parameter that determines the performance is *Euclidean Distance* (ED) rather than *Hamming Distance* (HD). The technique of "mapping by set partitioning" is introduced in [8]. This ensures that parallel transitions in the trellis code mapped into the signals are far enough in the signal constellation. Therefore, the probability of error is minimized. Since the design criteria for TCM is helpful only for AWGN channel, it usually causes a low diversity order, hence performance of TCM over fading channels is significantly degraded. To increase diversity order of TCM , symbol interleavers were used [9]. The design of TCM schemes to counteract simultaneously flat fading and AWGN was proposed in [10].

Zehavi suggested *Bit-interleaved Coded Modulation* (BICM) for fading channels which a coded system is built by a convolutional encoder followed by an interleaver and modulator[11]. Specifically, he suggested a system consisting of 8 states with rate $\frac{2}{3}$ convolutional code and three binary random interleavers. Outputs of interleavers are grouped and mapped to one of the symbols chosen from 8-PSK constellation using Gray mapping. Using random interleaver, higher diversity order can be achieved with the proposed system [11] compared to previous works. Thus BICM systems are quite

attractive for transmitting over fading channels. In [11], it is proven that the diversity order can be increased to the minimum number of distinct bits between two codewords rather than the number of distinct symbols which is suggested in [12]. The comparison between BICM (using bit interleaver) and TCM (using symbols interleaver) shows that BICM system outperforms TCM by one dB at the *Bit Error Rate* (BER) of 10^{-5}.

The general theoretical framework of Zehavi's concept is provided in [13] and a modified BICM model is proposed where all outputs of coded bits are fed into a single bit interleaver. It is shown in [13] that separation of demodulation and decoding is beneficial, since the encoder and the modulator can be chosen flexibly. Hence, by choosing the best convolutional code, which gives the largest Hamming distance for given code rate and constraint length, the diversity order can be maximized.

After introduction of Turbo codes [2], iterative decoding was applied to the bit-interleaved coded modulation systems and is called Bit-Interleaved Coded Modulation systems with Iterative Decoding (BICM-ID). The idea of iteration between decoder and demodulator is studied in [14] to overcome the drawback of conventional BICM systems. In [14], a simple iterative decoding with hard decision feedback is proposed. It was shown in [15] that BICM-ID significantly outperform the conventional TCM and is comparable to turbo TCM (TTCM) [16] over both Gaussian and Rayleigh fading channels with much less complexity. Requiring only one *soft-input soft output* (SISO) decoder instead of two as normally used in turbo decoding, is the advantage of BICM-ID over TTCM [2][16].

In response to increasing demand for using wireless communication systems and

more reliable services while the radio spectrum is limited, *Multiple Input Multiple Output*(MIMO) systems was introduced. This advanced technology promises significant improvement in spectral efficiency and as a result in system capacity [5][6]. MIMO systems make use of multiple transmit and receive antennas to improve the data rate by increasing the channel capacity and error performance over fading channels by increasing the diversity [17][18][19].

Utilizing multiple antennas at both transmitter and receiver sides allows high data rates as well as reliable communication. Hence multiple input multiple output (MIMO) systems are still an interesting topic in both industrial and academic fields. The potential for wide capacity gains was first addressed in [5]. Data rate over MIMO channels can be increased by various spatial multiplexing schemes [20]. For example, in *V-BLAST* (Vertical-Bell Labs Layered SpaceTime) architecture, independent data streams are transmitted in parallel over transmit antennas [21][22][23]. However, spatial multiplexing gain often results in a loss in spatial diversity [24].

Bit interleaved coded modulation schemes(BICM) for MIMO systems have recently been addressed as an effective mean to achieve high data rates while maintaining high diversity. It was shown in [25] that with a maximum-likelihood (ML) receiver, MIMO-BICM systems outperform spacetime trellis codes in fast fading channels. Employing BICM with iterative decoding (BICM-ID) over MIMO channels is proposed in [26], which improves BER performance significantly.

It has been shown that when signal constellation, interleaver and error control code are fixed, signal mapping has a crucial influence on the error performance of a BICM-ID system [15][27][28][29]. Similarly, the role of the signal mapping also applies to the error performance of MIMO-BICM-ID systems. This motivates us to study

the costellation/mapping designs for MIMO-BICM-ID systems.

1.2 Contributions

Since the signal constellation/mapping has a critical influence on the performance of BICM-ID systems, we focus on the constellation/mapping design over MIMO channels. In this thesis, multi-dimensional constellations/mappings are proposed for MIMO-BICM-ID systems. These constellations/mappings can improve the error performance of the system significantly due to optimization of the Euclidean distance between signal points.

First, a design criterion for multi-dimensional constellation/mapping is proposed based on minimization of pair-wise error probability. To reduce the complexity of exhaustive search, Binary Switching Algorithm (BSA)[30] is modified to find the optimal constellations/mappings. Based on these, several optimal constellations/mappings are obtained for 2-dimensional and 3-dimensional cases. Mutual information is used as a good measure to evaluate proposed signal constellations/mappings. New expression regarding discrete values is proposed to approximate the mutual information. Many simulations regarding mutual information have been done for different constellations/mappings. Based on simulation results comparison is made between proposed and conventional constellations and mappings.

Based on new constellation/mapping schemes, a transmitter is designed with multiple transmit antennas. A receiver is designed based on iterative decoding and ML detection. The receiver benefits using multiple antennas. Due to the exponentially growing complexity of the optimal Maximum-Likelihood (ML) detector, List Sphere Decoder (LSD) [31][32][33] is applied as the inner detector at the receiver.

Contributions are detailed in point form as follows:

- Multi-dimensional constellation concept for MIMO-BICM-ID systems is proposed.
- Design criteria for multi-dimensional signaling is suggested.
- Different mapping Schemes for 2-dimensional and 3-dimensional cases are illustrated.
- Mutual information expression is modified for simulating multi-dimensional signaling.
- Simulations for 2-dimensional QPSK, 2-dimensional 8QAM and 3-dimensional QPSK over AWGN and flat fading channels are performed.
- Proposed mappings are compared with conventional ones showing significant improvement on system performance.

1.3 Organization of Thesis

This thesis in organized in five chapters.

Chapter 2 studies bit-interleaved coded modulation (BICD) and BICM with iterative decoding for *single input single output* (SISO) channels. The influence of signal mapping on the error bounds is discussed. It is shown that for a fixed convolutional code and signal constellation, signal mapping plays a crucial role in determining the error performance. MIMO channels are studied and MIMO systems using BICM-ID concept are reviewed. In addition, Sphere Decoder and List Sphere Decoder algorithms are described, which will be used in our proposed receiver.

In Chapter 3, Multi-dimensional mapping for MIMO-BICM-ID transmitter system is introduced. The design criteria for this mapping scheme is explained. Design goal is to minimize Bit Error Rate (BER) by using pairwise error probability under the assumption of perfect *a priori* information at the demodulator/demapper. Mutual information is modified and new expression for discrete values is proposed which is used for simulations. At the end, some examples are provided and evaluated based on mutual information.

In Chapter 4, the focus is to design a receiver which is counterpart of the transmitter proposed in Chapter 3. The receiver performs based on iterative decoding. The detector/demapper is designed according to the multi-dimensional constellation proposed in Chapter 3. The modified detector/demapper works based on LSD.

Finally Chapter 5 concludes this thesis. Some future works are introduced in this chapter as well.

Chapter 2

Background

In communication systems, fading is caused by interference between two or more multi-path waves of the transmitted signal which arrive at the receiver at slightly different times. In multi-path fading environment, correlation between sequential fading coefficients degrades the error performance. The key parameter in determining error performance of any communication system over fading channel is diversity order [9]. In TCM systems, to reduce the correlation between fading coefficients symbol interleavers can be used [10]. Using symbol interleaver, the diversity order will be limited to the minimum number of distinct symbols between any two codewords. Thus, diversity can be increased by avoiding parallel transitions and increasing the constraint length of the code. Zehavi suggested *Bit-interleaved Coded Modulation* (BICM) for fading channels. The BICM system is built by a convolutional encoder followed by an interleaver[11]. The comparison between BICM (using bit interleaver) and TCM (using symbols interleaver) shows that BICM system outperforms TCM by one dB at the bit error rate of 10^{-5}.

2.1 Bit Interleaved Coded Modulation (BICM)

2.1.1 The BICM System Model

A conventional BICM system is a serial concatenation of information source, convolutional encoder, bit interleaver and M-ary modulator. Such a system is depicted in Fig. 2.1(a). Information bits **b** are encoded to produce **c**. Coded bits **c** are passed

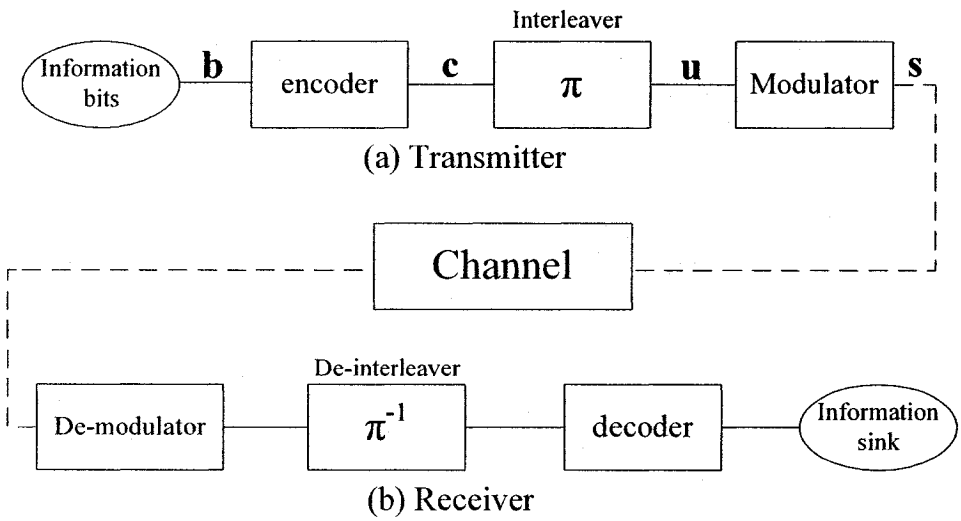

Figure 2.1: The BICM transceiver scheme

through a bit interleaver to produce **u**. Coded and interleaved bits are mapped to the appropriate constellation points according to the mapping scheme. Convolutional code is chosen to produce the largest Hamming distance d_H for the given code rate and constraint length. The pseudo-random interleaver permutes coded bits in order to position adjacent bits as far as possible. The interleaver is used to break the fading correlation and increase the diversity order to the minimum Hamming distance of the convolutional code. It should be noted that, in Fig. 2.1(a) only one interleaver is used instead of three separate interleavers which was Zehavi's original proposed scheme.

Using m bit interleaver limits the flexibility of BICM and complicates the analysis [13]. In addition, using three separate inteleavers cause a fixed correspondence between the output bits of the encoder and the label positions. This fixed correspondence results in unequal error protection and suboptimal performance when the code is chosen at random [13]. Then modulator input $\mathbf{u}$ is broken down into blocks of m bits. The k-th block is denoted as $\mathbf{u}_k = [u_{k,1}, u_{k,2}, ..., u_{k,m}]$. Each block of m bits is mapped to one of the signal points s_k chosen from M-ary constellation.

$$s_k = \mu(\mathbf{u}_k) = \mu(u_{k,1}, u_{k,2}, u_{k,3}) \tag{2.1}$$

where $\mu(.)$ denotes the mapping scheme. For a non-selective Rayleigh fading channel, the received signal can be written as,

$$r_k = a_k s_k + n_k \tag{2.2}$$

where r_k is the received signal at instance k, s_k is the transmitted signal, a_k is a Rayleigh random variable representing the fading coefficient of the transmitted signal s_k and n_k is the Additive White Gaussian Noise (AWGN) with zero mean and variance equal to $\frac{No}{2}$. It should be mentioned that the fading coefficient can be constant for few symbol duration (slow fading) or change from one symbol duration to another (fast fading).

The receiver of BICM consists of demodulator, de-interleaver and convolutional decoder. - Due to employing bit interleaver, joint demodulation and decoding for Maximum Likelihood (ML) detection of BICM is needed. Therefore, it is impractical due to complexity. In [11] Zehavi suggested a suboptimal method for decoding in two

separate stages: bit metric generation and Viterbi decoding [34]. From each received signal r_k, $2m$ log-likelihood bit metrics are produced, using ML rule. Considering one channel use, log-likelihood bit metrics can be expressed as,

$$\lambda(u_i) = \log P(r|u_i = b, a) \sim \log \sum_{s \in \Omega_b^i} P(r|s, a) \tag{2.3}$$

where Ω_b^i denotes the subset of constellation points whose label has the value b ("0" or "1") in its i-th position. The notation $\sim$ inicates the replacement by an equivalent statistic. The function $P(r|s, a)$ denotes the probability of receiving signal r given the signal s and fading coefficient a. This can be written as,

$$P(r|s, a) = \frac{1}{2\pi\sigma^2} \exp\left(-\frac{|r - as|^2}{2\sigma^2}\right) \tag{2.4}$$

where σ^2 is the noise variance. We can approximate equation (2.3) using log-sum approximation and equation (2.4) as follows,

$$\lambda(u_i) \sim \log \sum_{s \in \Omega_b^i} P(r|s, a) \approx \max_{s \in \Omega_b^i} \log P(r|s, a) = -\min_{s \in \Omega_b^i} |r - as|^2 \tag{2.5}$$

It means that, each bit metric is computed based on the minimum squared Euclidean distance between the received signal r and the signal point s over the subset $s \in \Omega_b^i$.

2.1.2 Signal Mapping Role Based on Error Bound of BICM

In this section, the influence of mapping on the BICM error performance based on error bounds, is reviewed .

Let $\mathbf{c}$ and $\hat{\mathbf{c}}$ denote the transmitted sequence and decoded sequence with Hamming distance d between them. $P(\mathbf{c} \longrightarrow \hat{\mathbf{c}})$ denotes the *pairwise error probability* (PEP). In other words, it is the probability of choosing $\hat{\mathbf{c}}$ instead of the transmitted sequence $\mathbf{c}$. The PEP of a BICM system, with ideal interleaving, is a function of the Hamming distance d between $\mathbf{c}$ and $\hat{\mathbf{c}}$,the labelling μ and the signal constellation Ω. Therefore, we can write PEP as,

$$P(\mathbf{c} \longrightarrow \hat{\mathbf{c}}) = f(d, \mu, \Omega) \tag{2.6}$$

The union bound of the BER for a BICM system using a rate $\frac{k_c}{n_c}$ convolutional code, a constellation Ω and a mapping μ is given by,

$$P_b = \frac{1}{k_c} \sum_{d=d_H}^{\infty} c_d f(d, \mu, \Omega) \tag{2.7}$$

where c_d is the total information weight of all error events at Hamming distance d and d_H is the free Hamming distance of the code [13].

In reference [13], it is mentioned that averaging over all sequences $\mathbf{c}$ and $\hat{\mathbf{c}}$ is impractical. Hence, a new tight bound called BICM expurgated bound for BICM systems is derived. Also, some insights into the asymptotic performance of BICM at high Signal to Noise Ratio (SNR) in given [13].

BICM performance is degraded over AWGN channel due to random modulation caused by interleaver. However, BICM performs well over Rayleigh fading channels. It is shown in [11] that, Free squared Euclidean Distance (FED) of BICM is given by

$$d_E^2 = d_H d_{min}^2 \tag{2.8}$$

where d_H is the free Hamming distance of a code and d_{min} is the smallest Euclidean

distance between the constellation points. For example in a 8PSK constellation $d_{min} = 2\sqrt{E_s}\sin(\frac{\pi}{8})$, where E_s is the symbol energy. It was shown that, generally the FED of BICM is a few dB lower than its counterpart TCM [11]. Hence, conventional BICM is less efficient than TCM for Gaussian channels.

In Rayleigh fading channels with perfect Channel State Information (CSI), the harmonic mean squared Euclidean distance determines the asymptotic performance of a BICM system and is defined as [13][15],

$$d_h^2(\mu) = \left(\frac{1}{m2^m} \sum_{i=1}^{m} \sum_{b=0}^{1} \sum_{s \in \Omega_b^i} \frac{1}{\|s - \hat{s}\|^2} \right)^{-1} \tag{2.9}$$

where $m = \log_2 M$, M is the size of constellation, and $\hat{s} \in \Omega_{\bar{b}}^i$ denotes the nearest neighbor of s. The asymptotic performance of BICM over Rayleigh fading channel is approximated by [13][15],

$$\log_{10} P_b \simeq -\frac{d_H}{10} \left[(R \cdot d_h^2(\mu))_{dB} + \left(\frac{E_b}{No} \right)_{dB} \right] + \text{constant} \tag{2.10}$$

where d_H is the minimum Hamming distance of the code and R is the data rate.

Another parameter which has influence on the error performance is introduced as distance spectrum of Euclidean distances for mappings with the value $N(d_E)$ [29]. It is defined as,

$$N(d_E) = \frac{1}{m2^m} \sum_{i}^{m} \sum_{b=0}^{1} \sum_{s_k \in \Omega_b^i} N_N(d_E, s_k) \tag{2.11}$$

where $N_N(d_E, s_k)$ is the number of symbols $\hat{s}_k \in \Omega_{\bar{b}}^i$ at Euclidean distance d_E of the symbol $s_k \in \Omega_b^i$, averaged over all bits $i = 1, 2, ..., m$ and 2^m symbols. The distance spectrum obviously depends on the specific mapping and should be as small

as possible.

Based on the error bound of BICM system, it can be observed that for a fixed error control code and fixed constellation, signal mapping has a significant effect on the error performance of the system. In [13] Gray and quasi-Gray mappings are proposed as optimal mappings for BICM systems.

2.2 Bit Interleaved Coded Modulation with iterative Decoding (BICM-ID)

In this section the system model of BICM with iterative decoding is discussed and the mapping role on the error performance of BICM is explained.

In the previous section, it was shown that BICM performs well over fading channels by increasing diversity order of the system. However, the performance of BICM is degraded over AWGN channels due to "random modulation" caused by interleaver. Therefore, conventional BICM systems are less efficient than TCM systems [11].

Recently, the success of turbo codes has shown the advantages of iterative processing in the decoding of concatenated coding schemes. Applying iterative decoding to BICM was studied in [35]. It is shown that BICM-ID with hard-decision feedback compares favorably with TCM over AWGN channels, while it significantly outperforms the BICM over fading channels.

In the BICM-ID, the feedback from robust data sections (i.e. less affected by noise or other channel impairments) can remove the ambiguity in the high orderd demodulation and enhance the decoding of weak data section (i.e. more affected data by noise). It is obvious that error in feedback leads us to choose the wrong constellation

point. Therefore, it is crucial to reduce the effect of feedback errors and control the error propagation. Hence, BICM-ID with soft-decision feedback and well-designed interleaver should be considered. We exclude the BICM-ID with hard-decision feedback from our studies. The following section discusses soft-decision BICM-ID receiver in more detail.

2.2.1 The BICM-ID System Model

The BICM-ID scheme is illustrated in Fig. 2.2. The transmitter performs exactly the same as BICM transmitter which was discussed in the previous section.

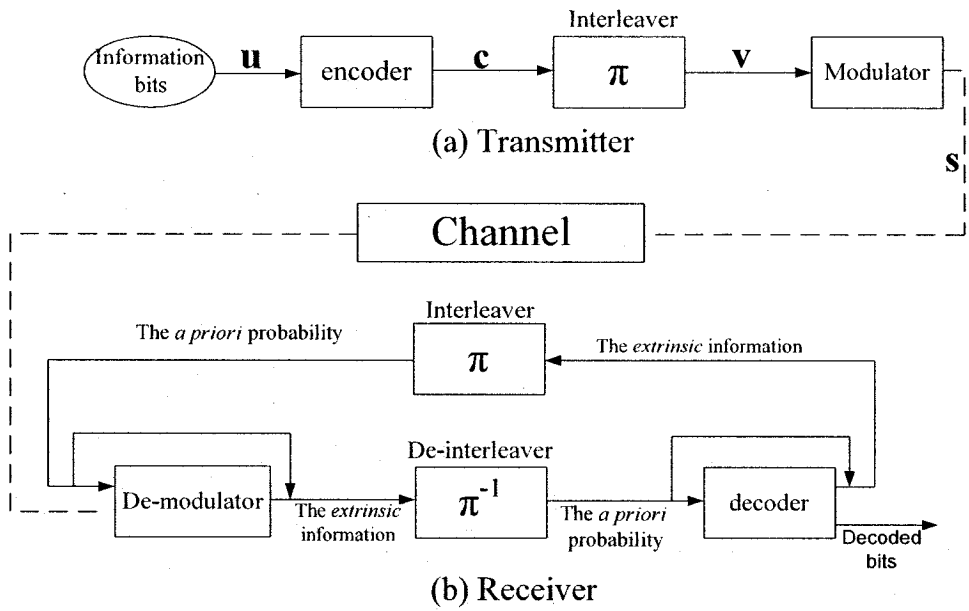

Figure 2.2: The BICM-ID transceiver scheme

As Fig. 2.2 shows, the receiver uses suboptimal iterative method. It utilizes two separate Soft-input Soft-output (SISO) components. Demodulator and decoder individually perform optimal. Fig. 2.3 illustrates the soft-decision receiver where,

the *a priori* information for the variable x is represented as $P(x;I)$ and *a posteriori* probability is denoted by $P(x;O)$. Demodulator generates *a posteriori* $P(v_k;O)$ information based on the received signal and the received *a priori* $P(v_k;I)$ information. It should be noted that, *a posteriori* information sometimes refers to as the *extrinsic* information in turbo code principle [2]. Then the deinterleaved *extrinsic* becomes *a priori* information $P(c_k;I)$ for the SISO decoder. The decoder generates *extrinsic* $P(c_k;O)$ information based on the received *a priori* information and trellis structure. This *extrinsic* information after interleaving becomes as *a priori* information $P(v_k;I)$ for the demodulator. For the first iteration, *a priori* information is not available and it is assumed that the transmitted signals are equally likely.

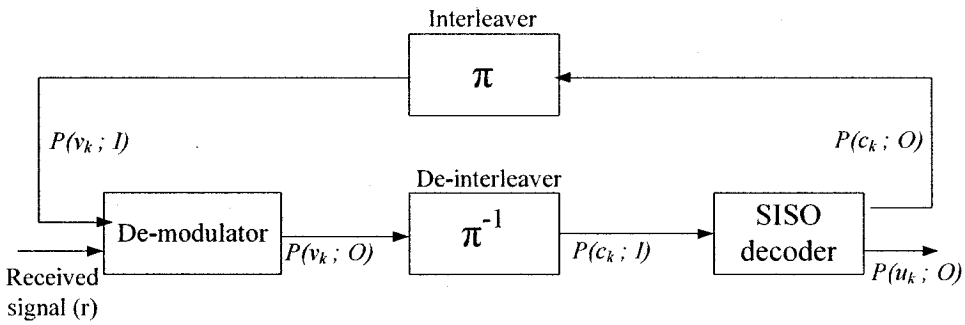

Figure 2.3: The receiver of BICM-ID system with soft-decision feedback

The *a posteriori* probability for the coded bits can be computed as,

$$P(v_k = b|r) \sim \sum_{s \in \Omega_b^i} P(s|r) \sim \sum_{s \in \Omega_b^i} P(r|s)P(s) \tag{2.12}$$

where v_k is the k-th bit in the signal label and Ω_b^i is the subset of constellation symbols that have b ("0" or "1") in their labels i-th position. $P(s)$ is the *a priori* probability of symbol s.

Using proper interleaving, m bits of the symbol label are independent. Therefore, the *a priori* information of the symbol s can be written as,

$$P(s) = \prod_{i=1}^{m} P(v_i = v_i(s); I) \tag{2.13}$$

where $v_i(s) \in \{0, 1\}$ is the value of i-th bit in the symbol s label. Using equations (2.12) and (2.13), the *extrinsic* information which is generated by the demodulator can be written as,

$$\begin{aligned} P(v_k = b; O) = \frac{P(v_k = b|r)}{P(v_k = b|I)} &= \frac{\left(\sum_{s \in \Omega_b^i} P(r|s)P(s)\right)}{P(v_k = b|I)} \\ &+ \sum_{s \in \Omega_b^i} \left(P(r|s) \prod_{i \neq k} P(v_i = v_i(s); I) \right) \end{aligned} \tag{2.14}$$

Equation (2.14) indicates that the bit metrics for one bit is calculated from the *a priori* probabilities of the other bits in the same symbol. The final decoded output is made at the final iteration based on extrinsic information $P(u_k; O)$. This information is also the *total a posteriori* probability since $P(u_k; I)$ is not used [15].

The interleaver design is critical to achieve high performance in BICM-ID systems. The interleaver should be designed to increase free squared Euclidean distance conditioned on the ideal feedback (FEDC) and to mitigate error propogation during iterative decoding.

2.2.2 Signal Mapping Role Based on Error Bound of BICM-ID

Signal mapping has the crucial effect on the error performance of BICM-ID systems. This influence can be evaluated by two Euclidean distances, which are the harmonic mean distance d_h^2 and harmonic mean distance with perfect knowledge about other bits $\tilde{d}_h^2$. The harmonic mean distance d_h^2 for any M-ary constellation, can be calculated as follows,

$$d_h^2 = \left(\frac{1}{m2^m} \sum_{i=1}^{m} \sum_{s \in \Omega_b^i} \frac{1}{|s - \hat{s}|^2} \right)^{-1} \tag{2.15}$$

where $m = \log_2 M$ and Ω_b^i denotes the constellation symbols whose labels have the value b ("0" or "1") in their i-th position. The symbol $\hat{s}$ in equation (2.15) belongs to $\Omega_{\bar{b}}^i$ where $\bar{b}$ is the compliment of b. $\hat{s}$ is the nearest neighbor of s. The harmonic mean distance with perfect knowledge about other bits $\tilde{d}_h^2$ can be computed by,

$$\tilde{d}_h^2 = \left(\frac{1}{m2^m} \sum_{i=1}^{m} \sum_{s \in \Omega_b^i} \frac{1}{|s - \tilde{s}|^2} \right)^{-1}. \tag{2.16}$$

where $\tilde{s} \in \Omega$ has the same label as s except at the i-th position.

The distance d_h^2 affects the asymptotic performance of the BICM while $\tilde{d}_h^2$ affects the asymptotic performance of the BICM-ID. The asymptotic performance of the BICM-ID system is defined as [28],

$$\log_{10} P_b \simeq -\frac{d_H}{10} \left[(R \cdot \tilde{d}_h^2(\mu))_{dB} + \left(\frac{E_b}{No} \right)_{dB} \right] + \text{constant} \tag{2.17}$$

where P_b is the probability of bit error, d_H is the minimum Hamming distance of

the convolutional code and R is the data rate. From equation (2.17), it can be observed that the code and the mapping have independent impacts on the asymptotic performance. Therefore, for a fixed convolutional code, a mapping should be chosen that maximizes $\tilde{d}_h^2$ while still a large enough d_h^2 is needed to make the first iteration work [28].

2.3 MIMO Channel Model

In wireless communication, due to surrounding environment different two or more multi-path waves of the transmitted signal arrive at the receiver at slightly different times. When these signals are arrived at the receiver, they may add constructively or destructively depending on the random phases of the signals arriving at the receiver. This phenomenon is known as fading. Fading can be characterized as frequency non-selective fading and frequency selective fading. In the flat fading channels, the transmitted signal bandwidth is smaller than the coherence bandwidth of the channel. In frequency selective fading, the transmitted signal bandwidth is larger than channel bandwidth. This causes different frequency components in the transmitted signal experience different fading attenuation. Therefore, the received signal is a distorted version of transmitted signal.

Fading can also been characterized as fast or slow fading. This definition is based on how rapidly channel changes regarding the transmitted signal duration [36]. The envelope of the received signal can be described as Rayleigh distribution or Ricean distribution.

In this thesis we only consider the Rayleigh flat fading channels. The channel is unknown for the transmitter but for the receiver it is perfectly known.

The MIMO channel with N_t transmit and N_r receive antennas is illustrated in Fig. 2.4. The channel path connecting antenna i to antenna j is modelled by a complex Gaussian distributed coefficient h_{ij} with $E[h_{ij}] = 0$ and $E[|h_{ij}|^2] = 1$, where $E[.]$ is the mathematical expectation. The path gains are collected to form an $N_r \times N_t$ *channel matrix* $\mathbf{H}[h_{ij}]$. The entries of channel matrix are assumed to be statistically independent.

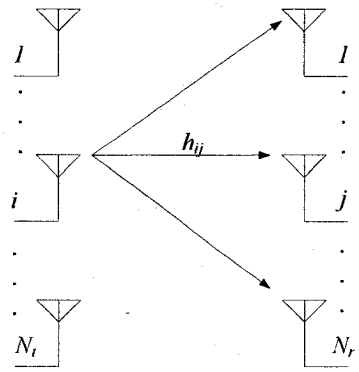

Figure 2.4: The MIMO channel

At time period k, the channel output is the superposition of the N_t transmitted symbols weighted by the corresponding path coefficient. This can be expressed as follows:

$$\mathbf{y}_k = \sqrt{\frac{P}{N_t}}\mathbf{H}_k\mathbf{s}_k + \mathbf{n}_k \tag{2.18}$$

where $\mathbf{y}_k = [y_{k1}, y_{k2}, ..., y_{kN_r}]^T$ is the received vector , $\mathbf{s}_k = [s_{k1}, s_{k2}, ..., s_{kN_t}]^T$ is the transmitted signal vector and $\mathbf{n}_k = [n_{k1}, n_{k2}, ..., n_{kN_r}]^T$ is the additive white Gaussian noise vector with zero mean and variance $\sigma^2 = N_o\mathbf{I}_{N_r}$. P is the total tranmit power over N_t antennas.

Traditionally fading was viewed as a disadvantage to the wireless system. But,

with the progressing of MIMO systems, it is thought that fading can be beneficial. This is because fading increases the degrees of freedom available for communication. This is indicated by the capacity of the ergodic MIMO channel with N_t transmit and N_r receive antennas which can be expressed as [6][5],

$$C(SNR) = E\left[\log\det(\mathbf{I}_{N_t} + \frac{SNR}{N_t}\mathbf{H}\mathbf{H}^H)\right] \tag{2.19}$$

$$C(SNR) \approx \min(N_t, N_r)\log\left(\frac{SNR}{N_t}\right), \qquad \forall \quad \text{high SNR} \tag{2.20}$$

We observe that at high SNR, the channel capacity increases with SNR as $\min(N_t, N_r)\log\left(\frac{SNR}{N_t}\right)$ bits per channel use. It shows that the capacity grows linearly with the smaller of the numbers of transmit and receiver antennas in rich scattering environments [5][6][20]. Moreover, using MIMO systems, the reliability is increased due to diversity. For a MIMO system with N_t transmit and N_r receive antennas, assuming that the path gains between two individual antennas are independently Rayleigh faded, the achievable maximal diversity gain is $N_t \times N_r$ [17][18][19][37][38][39]. Bell-Lab Layered Space-Time (BLAST) system is one of the practical space-time schemes that offers high spectral efficiency through its use of multiple antennas. The original BLAST is the D-BLAST (diagonal-BLAST) proposed by Foschini [40]. D-BLAST system offers efficient spatial diversity in expense of a high implementation complexity due to the use of specialized inter-substream block coding. V-BLAST (Vertical Bell-Lab Layered Space-Time) overcomes this limitation by excluding inter-substream block coding [21][22][23]. Thus V-Blast does not utilize spatial diversity. V-Blast method can be interpreted as spatial multiplexing.

2.4 Bit Interleaved Coded Modulation for MIMO

Multiple-input Multiple-output channels promise high improvement in the spectral efficiency of the system [5][6][20]. Combining MIMO systems with BICM and *a posteriori* (APP) decoding, makes this technique more efficient. This combination is studied in [26]. Fig 2.5 depicts the transmitter for such a system. The transmitter performs in the same fashion as BICM which is discussed in 2.1.1. Using a serial to parallel (S/P) component after the modulator, symbols are transmitted over N_t different transmit antennas. In other words, at each channel use the symbol vector $\mathbf{s} = [s_1, s_2, ..., s_{N_t}]^T$ which is a function of $N_t \times m$ bits ($m = \log_2 M$ and M is the constellation size) will be transmitted.

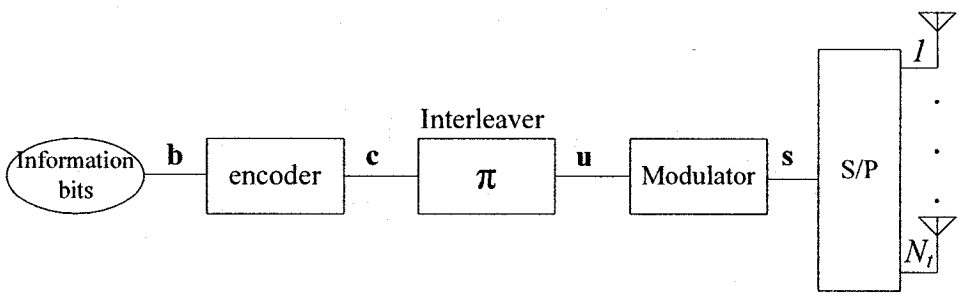

Figure 2.5: The transmitter of BICM for MIMO system

To recover the information bits, soft information of the coded bits needs to be extracted from the received signals. In iterative receivers, such as BICM-ID, usually a detector provides the receive symbol and using *a priori* information, the *a posteriori* (AAP) information is computed. The receiver of BICM for MIMO system is shown in Fig. 2.6.

Since coded bits have been randomly interleaved, it is possible to compute the probability of $c_j = b$ where $b \in \{0, 1\}$. This probability is called *a posteriori* and can

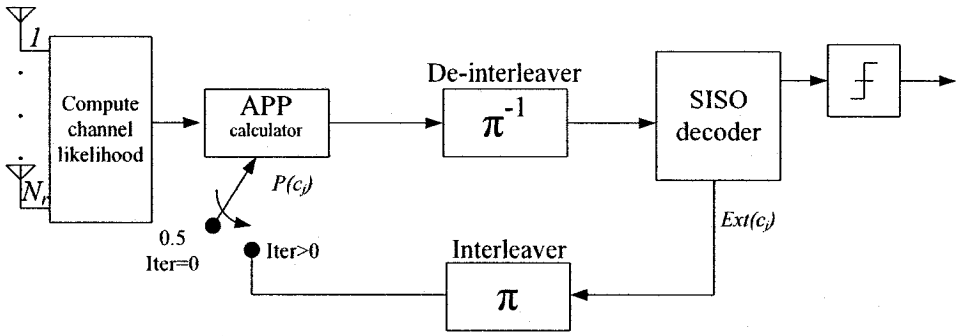

Figure 2.6: The receiver of BICM for MIMO system

be expressed as,

$$\begin{aligned} APP(c_j) &= p(c_j|\mathbf{y}) \\ &= \frac{P(\mathbf{y}|c_j).p(c_j)}{p(\mathbf{y})}, \qquad j = 1, ..., N_t \times m \end{aligned} \tag{2.21}$$

where $\mathbf{y}$ is the received vector which is described by equation (2.18) and $p(c_j)$ is the *a priori* information. The conditional probability of the bit c_j is determined by marginalizing the joint density of all bits. This can be expressed as,

$$\begin{aligned} P(\mathbf{y}|c_j) &= \sum_{c_i \in \{0,1\}, i=1,...,N_t \times m, i \neq j} P(\mathbf{y}, c_1, c_2, ..., c_{N_t \times m}|c_j) \\ &= \sum_{c_i \in \{0,1\}, i=1,...,N_t \times m, i \neq j} P(\mathbf{y}|c_1, c_2, ..., c_{N_t \times m}) \prod_{l \neq j} P(c_l) \end{aligned} \tag{2.22}$$

An essential part of calculation of APP is computing the likelihood function $P(\mathbf{y}|c_1, c_2, ..., c_{N_t \times m})$ and assuming $\mathbf{c} = [c_1, c_2, ..., c_{N_t \times m}]$. The APP can be found easily from the equation (2.18) as,

$$P(\mathbf{y}|\mathbf{s} = map(\mathbf{c})) = \frac{\exp\left(-\frac{1}{2\sigma^2} \cdot \|\mathbf{y} - \mathbf{Hs}\|^2\right)}{(2\pi\sigma^2)^{N_t}} \tag{2.23}$$

where σ^2 in the noise variance.

This information is passed through an interleaver and then processed by a SISO decoder. The SISO decoder produces an *extrinsic* information $Ext(c_j)$. This information after interleaving becomes *a priori* probability $P(c_j)$ for the coded bits c_j. This exchange of information continues until final iteration. The final decision is made based on *a posteriori* probability generated by the SISO decoder at the last iteration and $b_i = 0$ if $APP(b_i = 0) > APP(b_i = 1)$ otherwise $b_i = 1$.

2.5 Sphere Decoder

For detecting the received signal in MIMO systems, the *maximum a posteriori* (MAP) is one of the decision rules and is defined as,

$$\hat{s} = \arg\max_{\mathbf{s}\in\Omega}\{P(\mathbf{s}|\mathbf{y})\} \tag{2.24}$$

where Ω is the constellation.

Another decision rule is *Maximum Likelihood* (ML) rule which can be expressed as,

$$\hat{s} = \arg\min_{s\in\Omega}\{\|\mathbf{y} - \mathbf{Hs}\|^2\} \tag{2.25}$$

In other words, ML method chooses the symbol at the nearest distance to the received signal. In fact ML rule is equivalent to MAP rule if the transmitted signals

are equally likely.

It is shown that the best approach for detecting received signals is Maximum Likelihood (ML) detection approach [41]. ML promises the optimal performance. In the ML approach all the constellation points are checked to find the one which satisfies the equation (2.25). The major concerns in detecting usin ML approach, is the complexity. The complexity is growing exponential with the size of constellation. Therefore, ML detection is not feasible. For example, if a 8×8 MIMO system and 16QAM constellation is used, the ML detector needs to search over $16^8 \approx 4 \times 10^9$ symbols.

To make its use possible, the ML detection algorithms with reduced complexity have been proposed, such as the Sphere Decoding algorithm. SD is first proposed in [32] and expanded to MIMO systems in [31].

We try to search over only constellate points that lie in a fixed sphere of radius d around the given vector x. This idea is illustrated in Fig. 2.7

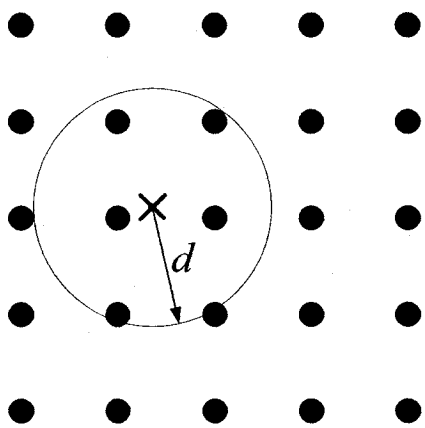

Figure 2.7: Idea of Sphere Decoding

Choosing the radius is one of the major concerns in using SD. If the radius d is chosen to be too small, only a few points will be found inside the sphere, this reduces the method performance. On the other hand if d is chosen to be too large, sphere contains many points and this slows down the SD detection.

Note that $\|n\|^2 = \|\mathbf{x} - \mathbf{Hs}\|^2$ is a χ^2 random variable with n degree of freedom. In fact the radius is a linear function of the noise variance, Therefore

$$d^2 = \alpha n \sigma^2 \tag{2.26}$$

where α is the tuning parameter and trying to satisfy $P(\|n\|^2 \leq d^2) = 1 - \epsilon (1 - \epsilon$ is set to be very close to 1). α can be achieved by solving the following equation,

$$\int_0^{\frac{\alpha n}{2}} \frac{\lambda^{\frac{n}{2}-1}}{\Gamma(\frac{n}{2})} e^{-\lambda} d\lambda = 1 - \epsilon \tag{2.27}$$

In the following, the general Sphere Decoding method is described [33].

It is assumed that channel matrix $\mathbf{H}$ is known perfectly at the receiver. The constellation point $\mathbf{Hs}$ lies inside a sphere of radius d centered at $\mathbf{x}$ if and only if

$$\|\mathbf{x} - \mathbf{Hs}\|^2 \leq d^2. \tag{2.28}$$

QR factorization of the matrix H is used in order to make the equation (2.28) easier to be solved.

$$\mathbf{H} = \mathbf{Q} \begin{bmatrix} \mathbf{R} \\ 0_{(n-m)\times m} \end{bmatrix} \tag{2.29}$$

where $\mathbf{R}$ is an $m \times m$ upper triangular matrix, and $\mathbf{Q} = [\mathbf{Q}_1 \mathbf{Q}_2]$ is an $n \times n$ orthogonal matrix. The matrices $\mathbf{Q}_1$ and $\mathbf{Q}_2$ represent the first m and last $n - m$ orthogonal

columns of $\mathbf{Q}$, respectively. We can rewrite the equation (2.28) using equation (2.29), as follows

$$\begin{aligned} d^2 &\geq \left\| \mathbf{x} - [\mathbf{Q}_1 \quad \mathbf{Q}_2] \begin{bmatrix} \mathbf{R} \\ 0 \end{bmatrix} s \right\|^2 = \left\| \begin{bmatrix} \mathbf{Q}_1^H \\ \mathbf{Q}_2^H \end{bmatrix} \mathbf{x} - \begin{bmatrix} \mathbf{R} \\ 0 \end{bmatrix} \mathbf{s} \right\|^2 \\ &= \|\mathbf{Q}_1^H \mathbf{x} - \mathbf{R}\mathbf{s}\|^2 + \|\mathbf{Q}_2^H \mathbf{x}\|^2 \end{aligned} \tag{2.30}$$

where $(.)^H$ denotes Hermitian matrix transposition. Equation (2.30) can be rewritten as,

$$d^2 - \|\mathbf{Q}_2^H \mathbf{x}\|^2 \geq \|\mathbf{Q}_1^H \mathbf{x} - \mathbf{R}\mathbf{s}\|^2 \tag{2.31}$$

Defining $y = Q_1^H x$ and $\acute{d}^2 = d^2 - \|Q_2^H x\|^2$, we can rewrite the last equation as,

$$\acute{d}^2 \geq \sum_{i=1}^{m} \left(y_i - \sum_{j=1}^{m} r_{i,j} s_j \right)^2 \tag{2.32}$$

where $r_{i,j}$ denotes an (i,j) entry of the R. Using the upper triangular property of R, we can rewrite equation (2.32) as follows,

$$\begin{aligned} \acute{d}^2 &\geq (y_m - r_{m,m} s_m)^2 \\ &\quad + (y_{m-1} - r_{m-1,m} s_m - r_{m-1,m-1} s_{m-1})^2 + ... \end{aligned} \tag{2.33}$$

It can be observed that in equation (2.33), the first term depends only on s_m, the second term on $\{s_m, s_{m-1}\}$ and so on. Therefore, $\acute{d}^2 \geq (y_m - r_{m,m} s_m)^2$ is a necessary condition for $\mathbf{Hs}$ to be enclosed in the sphere. This inequality can be written in the following form,

$$\left\lceil \frac{-\acute{d}^2 + y_m}{r_{m,m}} \right\rceil \leq s_m \leq \left\lfloor \frac{\acute{d}^2 + y_m}{r_{m,m}} \right\rfloor \tag{2.34}$$

where $\lceil . \rceil$ denotes rounding to the nearest larger elements in the set of numbers that spans the lattice. Similarly, $\lfloor . \rfloor$ denotes rounding to the nearest smaller elements in the set of numbers that spans the lattice.

For each s if s_m satisfies equation (2.34) then the next dimension s_{m-1} should be checked. The radius for the next dimension can be defined as

$$\acute{d}^2_{m-1} = \acute{d}^2 - (y_m - r_{m,m}s_m)^2 \tag{2.35}$$

and considering

$$y_{m-1|m} = y_{m-1} - r_{m-1,m}s_m \tag{2.36}$$

simplifies the calculations in the next dimension. Therefore, s_{m-1} belongs to

$$\left\lceil \frac{-\acute{d}^2_{m-1} + y_{m-1|m}}{r_{m-1,m-1}} \right\rceil \leq s_{m-1} \leq \left\lfloor \frac{\acute{d}^2_{m-1} + y_{m-1|m}}{r_{m-1,m-1}} \right\rfloor \tag{2.37}$$

This progress will be continued untill s_1. Thus, all constellation points belonging to (2.28) are obtained. The formalized algorithm can be found in [33].

Chapter 3

Constellation Mapping Optimization for MIMO-BICM-ID

It has been shown that when signal constellation, interleaver and error control code are fixed, signal mapping has a crucial influence on the error performance of a BICM-ID system [15][27][28][29]. Recently, Multi-dimensional mapping has been proposed in [42][43] for Single-Input Single-Output BICM-ID systems.

To maximize the gain of iterative decoding, we make crucial changes to traditional mappings. In this chapter, Multi-dimensional mapping for MIMO-BICM-ID systems is introduced. The design criteria for this mapping scheme is explained. Design goal is to minimize BER by using pairwise error probability under the assumption of perfect *a priori* information at the demodulator/demapper. At the end, some examples are provided and evaluated based on mutual information.

3.1 System Model

In this thesis, we consider the BICM-ID system using multiple transmitter antenna depicted in Fig. 3.1. The transmitter is a serial concatenation of the information source, an encoder, a bit-interleaver (π), a serial to parallel convertor and a Multi-Dimensional mapper. The information bits $\mathbf{b}$ are first encoded by an outer convolutional encoder of rate R_c to produce the output coded bit sequence. The convolutional code is chosen to be optimal in the sense that it gives the largest free Hamming distance d_H for given code rate and constraint length. The coded bits are permuted randomly by the pseudo-random interleaver, the output sequence is $\mathbf{c}$.

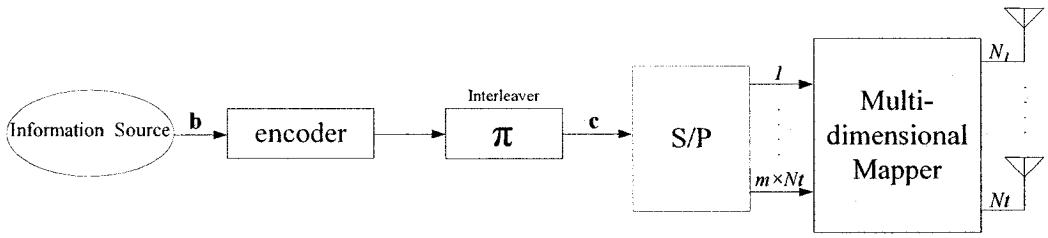

Figure 3.1: The transmitter of MIMO-BICM-ID.

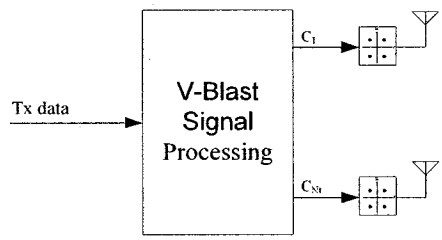

Figure 3.2: V-BLAST Transmitter

For conventional MIMO-BICM or to be more precise V-BLAST-BICM systems, a coded and interleaved bit sequence is demultiplexed into N_t sub-sequences. Then each sub-sequence bit stream is fed to its respective transmitter. At the transmitter

each $m = \log_2 M$ bits are mapped independently to one of the signal points chosen from an M-ary constellation. Hence at each time slot k, N_t different and independent signals will be sent over N_t transmit antennas as shown in Fig. 3.2 . In contrast to the conventional systems, in the proposed design, the sequence of N coded and interleaved bits, $[c_0, c_1, ..., c_{N-1}]$, is broken down into blocks of $m \times n$ bits, which m is the number of bits per conventional complex symbol and n is the number of dimension. It is assumed that the number of dimensions is equal to the number of transmit antennas. The k-th block is denoted as

$$\mathbf{c}_k = [c_{k0}, c_{k1}, ..., c_{k(m\times n-1)}] \tag{3.1}$$

where c_{ki} is a coded and interleaved bit which gets a value of either 0 or $1(0 \leq i \leq m \times n - 1)$, $1 \leq k \leq K$, and $K = \frac{N}{m\times n}$). Now $\mathbf{c}_k$ bits are simultaneously mapped to n parallel M-ary signal points ($n \times 1$ vector, where $n = N_t$). This will make a bigger constellation ϕ in n dimensions, having M^n signal points, where

$$\mathbf{s}_i = \mu(\mathbf{c}_k). \tag{3.2}$$

$\mu(\cdot)$ denotes the multi-dimensional mapping function, choosing one of the n-dimensional signals according to $m \times n$ bits. In proposed constellation each signal point can be represented as a vector:

$$\mathbf{s}_i = [x_{1,i}, x_{2,i}, ..., x_{n,i}]^T \tag{3.3}$$

where $x_{p,i}$, represents the p-th conventional $M - ary$ constellation point.

The main difference between conventional mapping scheme and our multi-dimensional

mapping is that in our scheme, choosing each symbol $x_{p,i} \in \Omega$, $1 \leq p \leq n$ is a function of $m \times n$ bits while in the conventional scheme it merely depends on m bits. It is clear that conventional mapping scheme can be a special case of our proposed one, when $n = 1$. On the other hand our scheme does not change spectrum efficiency.

We consider the transmission of data frame over a frequency-nonselective Rayleigh fading channel with N_t transmit antennas and N_r receive antennas. As a conventional multiple input multiple output (MIMO) system, the channel path connecting antenna i to antenna j is modeled by a complex Gaussian distributed coefficient h_{ij} with $E[h_{ij}] = 0$ and $E[|h_{ij}|^2] = 1$, where E[.] is the mathematical expectation. The path gains are collected to form an $N_r \times N_t$ *channel matrix* $\mathbf{H}[h_{ij}]$. The entries of channel matrix are assumed to be statistically independent.

At time period k, the channel output is the superposition of the N_t transmitted symbols weighted by the corespondent path coefficient. This can be expressed as follows:

$$\mathbf{y}_k = \mathbf{H}_k.\mathbf{s}_k + \mathbf{n}_k \tag{3.4}$$

where $\mathbf{y}_k = [y_{k1}, y_{k2}, ..., y_{kN_r}]^T$ is the received vector , $\mathbf{s}_k = [s_{k1}, s_{k2}, ..., s_{kN_t}]^T$ is the transmitted signals vector and $\mathbf{n}_k = [n_{k1}, n_{k2}, ..., n_{kN_r}]^T$ is the additive white Gaussian noise vector with zero mean and variance $\sigma^2 = N_o\mathbf{I}_{N_r}$.

In this thesis two types of channels are considered. The first type is *quasi-static Rayleigh fading* channel (block fading) where the channel maintains constant in one modulation block but it may change from block to block. Hence the channel is not necessarily constant for a coding frame which usually consists of a large number of

modulation blocks. The second type is *non-static Rayleigh fading* (fast fading) channel where the channel changes randomly and independently at each symbol period.

In this thesis to avoid increasing complexity we assume equal number of transmit and receive antennas (N_t=N_r).

3.2 Design Criterion for MIMO Mapping

In this section, we derive a criterion for optimal mapping based on *pairwise error probability* (PEP).

Let's $P(S_k \rightarrow \hat{S}_k)$ express the probability of choosing $\hat{S}_k$ instead of the actual transmitted signal S_k. $P(S_k \rightarrow \hat{S}_k)$ can be written as:

$$P(S_k \rightarrow \hat{S}_k) = \mathrm{Q}\left(\frac{d}{2\sigma_n}\right) \tag{3.5}$$

where σ_n^2 is variance of AWG noise and can be denoted as $\frac{N_o}{2}$. Hence we can rewrite equation 3.5 as:

$$P(S_k \rightarrow \hat{S}_k) = \mathrm{Q}\left(\frac{d}{\sqrt{2N_o}}\right) \tag{3.6}$$

where d is the Euclidean distance between S_k and $\hat{S}_k$. In a MIMO systems where channel matrix $\mathbf{H}$ is perfectly known in the receiver, d can be expressed as:

$$d = \sqrt{\|\mathbf{H}(S_k - \hat{S}_k)\|^2} \tag{3.7}$$

Hence the pairwise error probability (PEP) in equation (3.5) can be rewritten as:

$$P(S_k \rightarrow \hat{S}_k) = \mathrm{Q}\left(\frac{\sqrt{\|\mathbf{H}(S_k - \hat{S}_k)\|^2}}{2\sigma_n}\right) = \mathrm{Q}\left(\sqrt{\frac{\|\mathbf{H}(S_k - \hat{S}_k)\|^2}{2N_o}}\right) \tag{3.8}$$

An upper bound for Q-function is used, called Gaussian Tail approximation. It is derived from the chernoff bound [36] and states:

$$\mathrm{Q}(x) \leq \frac{1}{2}\exp(-\frac{x^2}{2}), \qquad x \geq 0. \tag{3.9}$$

The use of this bound in equation(3.8) gives:

$$P(S_k \rightarrow \hat{S}_k) \leq \frac{1}{2}\exp\left(-\frac{\|\mathbf{H}(S_k - \hat{S}_k)\|^2}{4N_o}\right) \tag{3.10}$$

3.2.1 Design Based on Pairwise Error Probability

Assume two codewords $\mathbf{c}$ and $\hat{\mathbf{c}}$ which differ in d bits (Hamming distance). Assuming ideal interleaving, these d different positions will be spread in space and time over d distinct transmission period. Let $P(\mathbf{c} \rightarrow \hat{\mathbf{c}})$ denotes pairwise error probability (PEP), i.e. choosing the sequence $\hat{\mathbf{c}}$ instead of transmitted sequence $\mathbf{c}$. This PEP can be achieved by averaging over all symbols defined by constellation and all bit positions(q) as it is determined in [13].

$$P(\mathbf{c} \rightarrow \hat{\mathbf{c}}) = \left\{\frac{1}{q \cdot 2^q}\sum_{i=1}^{q}\sum_{b=0}^{1}\sum_{s_k \in \phi_b^i}\sum_{\hat{s}_k \in \phi_{\bar{b}}^i} P(S_k \rightarrow \hat{S}_k)\right\}^d \tag{3.11}$$

where $\mathbf{s}_k \in \phi_b^i$ denotes symbols whose labels have the value $b \in [0,1]$ in their i-th position similarly, $\hat{\mathbf{s}}_k \in \phi_{\bar{b}}^i$ are symbols with $\bar{b}$ in their i-th position.

Obviously the pairwise error probabilities of symbol vectors with a small Euclidean distance dominate the overall error performance. This depicts the playing role of the mapping in error bounds.

Substituting equation (3.10) in (3.11) and considering number of bits in proposed multi-dimensional signal mapping, result in:

$$P(\mathbf{c} \rightarrow \hat{\mathbf{c}}) = \left\{ \frac{1}{nm \cdot 2^{nm+1}} \sum_{i=1}^{nm} \sum_{b=0}^{1} \sum_{s_k \in \phi_b^i} \sum_{\hat{s}_k \in \phi_{\bar{b}}^i} \exp\left(-\frac{\|\mathbf{H}(\mathbf{S}_k - \hat{\mathbf{S}}_k)\|^2}{4N_o} \right) \right\}^d \tag{3.12}$$

Based on PEP in equation (3.12) and considering the influence of Euclidean distance of pairwise symbols, the criteria to choose the best mapping can be defined as optimization of the cost function δ where

$$\delta = E_{\mathbf{H}} \left[\frac{1}{nm \cdot 2^{nm+1}} \sum_{i=1}^{nm} \sum_{b=0}^{1} \sum_{s_k \in \phi_b^i} \sum_{\hat{s}_k \in \phi_{\bar{b}}^i} \exp\left(-\frac{\|\mathbf{H}(\mathbf{S}_k - \hat{\mathbf{S}}_k)\|^2}{4N_o} \right) \right] \tag{3.13}$$

and $E_{\mathbf{H}}[\cdot]$ denotes mathematical expectation over channel matrix $\mathbf{H}$. Equation (3.13) can be rewrite as:

$$\delta = \frac{1}{nm \cdot 2^{nm+1}} \sum_{i=1}^{nm} \sum_{b=0}^{1} \sum_{s_k \in \phi_b^i} \sum_{\hat{s}_k \in \phi_{\bar{b}}^i} E_{\mathbf{H}} \left[\exp\left(-\frac{\|\mathbf{H}(\mathbf{S}_k - \hat{\mathbf{S}}_k)\|^2}{4N_o} \right) \right] \tag{3.14}$$

The result of the expectation in equation (3.14) will be different for AWGN, slow fading and fast fading channels. Considering slow fading situation and using the

procedure shown in [18], the criteria function is simplified as:

$$\delta = \frac{1}{nm \cdot 2^{nm+1}} \sum_{i=1}^{nm} \sum_{b=0}^{1} \sum_{\mathbf{s}_k \in \phi_b^i} \sum_{\hat{\mathbf{s}}_k \in \phi_b^i} \frac{1}{\frac{1}{4N_o} |\mathbf{S}_k - \hat{\mathbf{S}}_k|^2} \tag{3.15}$$

It should be noted that δ in equation (3.15) depends on the channel signal to noise ratio. On the other hand, δ depicts the signal mapping effect on the asymptotic performance of MIMO-BICM-ID systems, the smaller cost function (δ) the lower asymptotic bit error performance.

In the next chapter numerous simulations are performed for AWGN, slow fading and fast fading channels which show good performance for cases. The criteria obtained in equation (3.15) has been used as a general cost function to choose the mapping scheme over all kinds of channels in this thesis.

As it is mentioned, the derived criteria is based on pairwise error probability, in other words, the Euclidean distance between two symbols which are common in all bit positions except one is maximized. Therefore, we are intuitively using the genie method that assumes perfect a priori information [44].

An optimum mapping is the one that minimizes the cost function defined in equation (3.15). It is obvious that for a crowded constellation, an exhaustive search to find a mapping that yields the smallest values of the cost function, is impossible due to the complexity. To avoid long searches, we use Binary Switching Algorithm (BSA) in this thesis as explained in the next section.

3.3 Modified Binary Switching Algorithm

Binary Switching Algorithm (BSA) is proposed first in [30]. The main idea involves iteratively switching the index of two symbols to reduce the cost function (3.15). BSA starts with an initial mapping, using cost function (δ) in equation (3.15). Then cost of each symbol and the total cost corresponding to all symbols existing in the constellation are calculated. Afterwards, an ordered list of symbols sorted by the decreasing cost is generated. The symbol with the largest cost (the one with the strongest contribution to the poor performance) is selected as a candidate to be switched first. The label of this symbol is switched temporarily with the label of another symbol, and the total cost regarding the tentative switch recalculated. To determine the possible decrease in total cost following each switch. Eventually, a switch is selected such that the decrease of the total cost due to that change is as large as possible. If such a switch cannot be found (an unsuccessful switch attempt), then the symbol with the second highest cost is chosen to check for the possible decrease in total cost. This process is continued with all the symbols in the decreasing ordered list till a successful switch occur. Following each successful switch a new decreasing order list is generated and the process starts over. This will be continued until no further decreasing in total cost is possible due to switching the label of symbols. Then the algorithm halts in a locally optimal state.

Since the outcome of applying BSA is locally optimum, different initial mappings results in different output mappings. In other words, the output of the BSA is dependent on initial mapping. For initializing mapping the simplest method is to choose an arbitrary mapping. Applying several random initial mappings leads to the presumable global optimal mapping.

As noted previously, the default for the algorithm is to keep running until a local optimum is reached. In this case, if the index of two symbols are switched, then no decrease in (δ), can result. This halting condition can yield extremely long running times for crowded constellations. The other option is to define a poor upper bound on running time considering maximum number of index switches possible or define an upper bound for iteration[1] numbers. BSA procedure is described in Fig. 3.3.

In this thesis, our goal is to modify the conventional signal mapping in order to improve the error performance, therefore this mapping scheme is used as the BSA initial mapping. Then, the proposed mappings are evaluated as explained in the next section.

3.4 Proposed Mappings for MIMO-BICM-ID

In this section, improved mapping schemes for BICM-ID over MIMO systems is presented based on the design criteria introduced in the previous sections. It is assumed that the system operates over Rayleigh block fading channels.

In the following subsection the mapping for several kinds of signaling is presented; four signal mapping corresponding to 2-dimensional case and one for 3-dimensional. In 2-dimensional signaling three different kinds of well known conventional constellations QPSK, 8QAM and 8PSK are used. QPSK signaling is also used in 3-dimensional constellation. To increase the data rate more crowded constellations such as 16QAM and 32QAM can be used in the expense of adding complexity. The complexity will increase exponentially with increasing the constellation order.

[1]The completion of each switch or unsuccessful switch attempt constitutes the end of an iteration

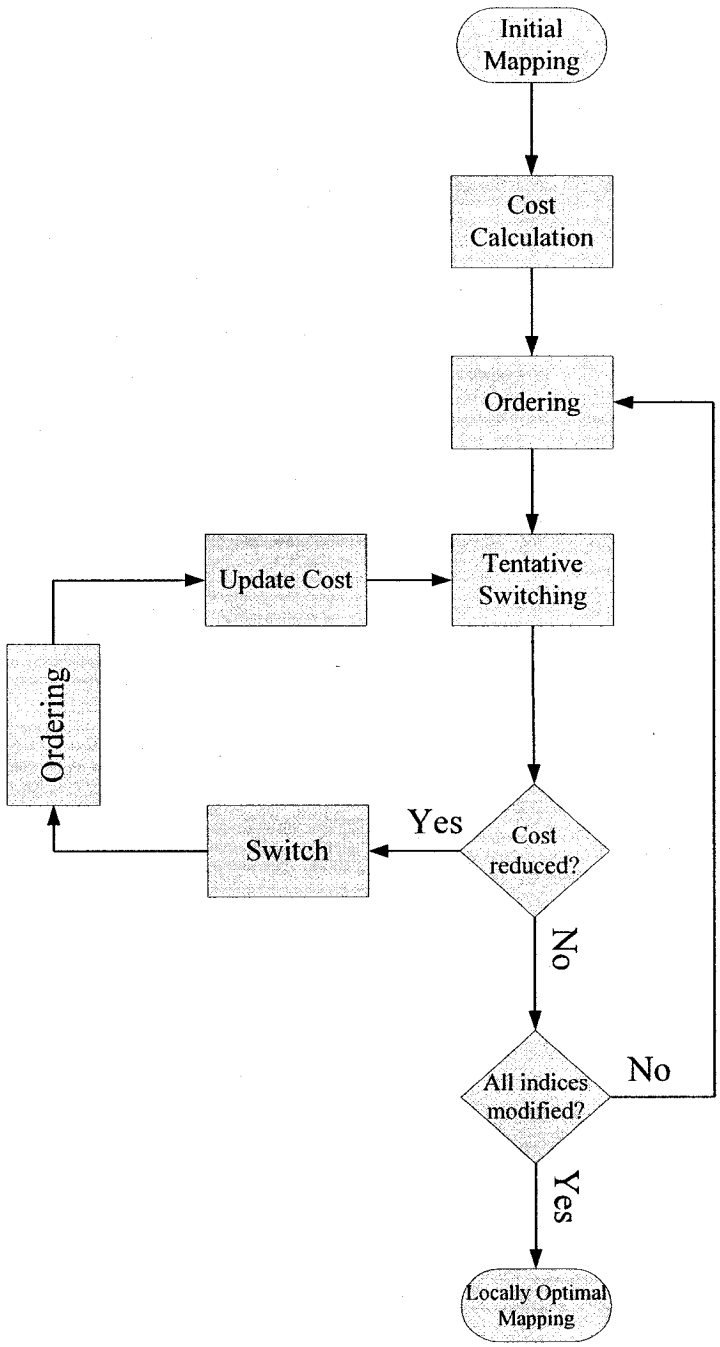

Figure 3.3: Binary Switching Algorithm(BSA) procedure block diagram

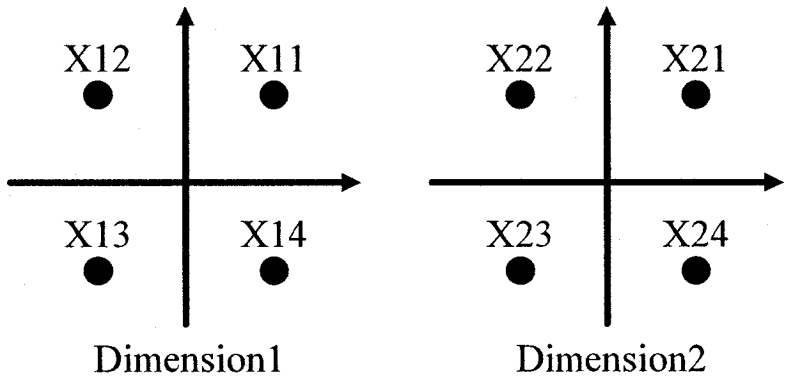

Figure 3.4: 2-dimensional QPSK constellation scheme

$X_{13}, X_{24} \rightarrow 1$	$X_{11}, X_{21} \rightarrow 2$	$X_{13}, X_{22} \rightarrow 3$	$X_{11}, X_{23} \rightarrow 4$
$X_{12}, X_{22} \rightarrow 5$	$X_{14}, X_{23} \rightarrow 6$	$X_{12}, X_{24} \rightarrow 7$	$X_{14}, X_{21} \rightarrow 8$
$X_{11}, X_{24} \rightarrow 9$	$X_{13}, X_{21} \rightarrow 10$	$X_{11}, X_{22} \rightarrow 11$	$X_{13}, X_{23} \rightarrow 12$
$X_{14}, X_{22} \rightarrow 13$	$X_{11}, X_{23} \rightarrow 14$	$X_{14}, X_{24} \rightarrow 15$	$X_{11}, X_{21} \rightarrow 16$

Table 3.1: The proposed mapping for 2-dimensional QPSK scheme

3.4.1 The proposed mapping schemes

In each multi-dimensional case, the required mapping can be obtained by minimizing the cost function δ as introduced in equation (3.15). Such mappings are found for 2-dimensional QPSK, 2-dimensional 8QAM, 2-dimensional 8PSK and 3-dimensional QPSK by computer search using BSA. The proposed mapping for 2-dimensional QPSK is depicted in Fig. 3.4 followed by table 3.1 which shows the index assignments for corresponding constellation.

The proposed mapping for 2-dimensional 8QAM is depicted in Figs. 3.5 and 3.6 followed by tables 3.2 and 3.3 which show the index assignments for corresponding constellations.

$X_{18}, X_{26} \rightarrow 1$	$X_{14}, X_{22} \rightarrow 2$	$X_{16}, X_{21} \rightarrow 3$	$XS_{11}, X_{24} \rightarrow 4$
$X_{15}, X_{23} \rightarrow 5$	$X_{11}, X_{28} \rightarrow 6$	$X_{11}, X_{27} \rightarrow 7$	$X_{16}, X_{26} \rightarrow 8$
$X_{15}, X_{22} \rightarrow 9$	$X_{11}, X_{25} \rightarrow 10$	$X_{18}, X_{23} \rightarrow 11$	$X_{13}, X_{27} \rightarrow 12$
$X_{12}, X_{27} \rightarrow 13$	$X_{16}, X_{23} \rightarrow 14$	$X_{14}, X_{26} \rightarrow 15$	$X_{11}, X_{22} \rightarrow 16$
$X_{13}, X_{21} \rightarrow 17$	$X_{18}, X_{25} \rightarrow 18$	$X_{16}, X_{25} \rightarrow 19$	$X_{12}, X_{28} \rightarrow 20$
$X_{18}, X_{22} \rightarrow 21$	$X_{13}, X_{26} \rightarrow 22$	$X_{14}, X_{28} \rightarrow 23$	$X_{18}, X_{24} \rightarrow 24$
$X_{12}, X_{26} \rightarrow 25$	$X_{16}, X_{22} \rightarrow 26$	$X_{13}, X_{28} \rightarrow 27$	$X_{17}, X_{24} \rightarrow 28$
$X_{15}, X_{24} \rightarrow 29$	$X_{11}, X_{21} \rightarrow 30$	$X_{17}, X_{23} \rightarrow 31$	$X_{14}, X_{27} \rightarrow 32$
$X_{15}, X_{21} \rightarrow 33$	$X_{12}, X_{25} \rightarrow 34$	$X_{13}, X_{25} \rightarrow 35$	$X_{17}, X_{21} \rightarrow 36$
$X_{12}, X_{22} \rightarrow 37$	$X_{15}, X_{26} \rightarrow 38$	$X_{15}, X_{28} \rightarrow 39$	$X_{11}, X_{23} \rightarrow 40$
$X_{11}, X_{26} \rightarrow 41$	$X_{16}, X_{27} \rightarrow 42$	$X_{16}, X_{28} \rightarrow 43$	$X_{12}, X_{24} \rightarrow 44$
$X_{15}, X_{25} \rightarrow 45$	$X_{12}, X_{21} \rightarrow 46$	$X_{12}, X_{23} \rightarrow 47$	$X_{15}, X_{27} \rightarrow 48$
$X_{14}, X_{25} \rightarrow 49$	$X_{17}, X_{22} \rightarrow 50$	$X_{18}, X_{27} \rightarrow 51$	$X_{14}, X_{23} \rightarrow 52$
$X_{17}, X_{25} \rightarrow 53$	$X_{14}, X_{21} \rightarrow 54$	$X_{13}, X_{23} \rightarrow 55$	$X_{17}, X_{27} \rightarrow 56$
$X_{18}, X_{21} \rightarrow 57$	$X_{14}, X_{24} \rightarrow 58$	$X_{16}, X_{24} \rightarrow 59$	$X_{17}, X_{28} \rightarrow 60$
$X_{13}, X_{22} \rightarrow 61$	$X_{17}, X_{26} \rightarrow 62$	$X_{18}, X_{28} \rightarrow 63$	$X_{13}, X_{24} \rightarrow 64$

Table 3.2: The proposed mapping for 2-dimensional 8QAM scheme(1)

$X_{16}, X_{26} \rightarrow 1$	$X_{13}, X_{24} \rightarrow 2$	$X_{11}, X_{23} \rightarrow 3$	$X_{16}, X_{27} \rightarrow 4$
$X_{11}, X_{25} \rightarrow 5$	$X_{18}, X_{23} \rightarrow 6$	$X_{18}, X_{22} \rightarrow 7$	$X_{13}, X_{26} \rightarrow 8$
$X_{14}, X_{21} \rightarrow 9$	$X_{15}, X_{27} \rightarrow 10$	$X_{17}, X_{28} \rightarrow 11$	$X_{14}, X_{24} \rightarrow 12$
$X_{17}, X_{22} \rightarrow 13$	$X_{12}, X_{28} \rightarrow 14$	$X_{12}, X_{25} \rightarrow 15$	$X_{15}, X_{21} \rightarrow 16$
$X_{11}, X_{21} \rightarrow 17$	$X_{18}, X_{27} \rightarrow 18$	$X_{16}, X_{28} \rightarrow 19$	$X_{11}, X_{24} \rightarrow 20$
$X_{16}, X_{22} \rightarrow 21$	$X_{13}, X_{28} \rightarrow 22$	$X_{13}, X_{25} \rightarrow 23$	$X_{18}, X_{21} \rightarrow 24$
$X_{17}, X_{26} \rightarrow 25$	$X_{12}, X_{24} \rightarrow 26$	$X_{14}, X_{23} \rightarrow 27$	$X_{17}, X_{27} \rightarrow 28$
$X_{14}, X_{25} \rightarrow 29$	$X_{15}, X_{23} \rightarrow 30$	$X_{15}, X_{22} \rightarrow 31$	$X_{12}, X_{26} \rightarrow 32$
$X_{17}, X_{21} \rightarrow 33$	$X_{12}, X_{27} \rightarrow 34$	$X_{14}, X_{28} \rightarrow 35$	$X_{17}, X_{24} \rightarrow 36$
$X_{14}, X_{22} \rightarrow 37$	$X_{15}, X_{28} \rightarrow 38$	$X_{15}, X_{25} \rightarrow 39$	$X_{12}, X_{21} \rightarrow 40$
$X_{11}, X_{26} \rightarrow 41$	$X_{18}, X_{24} \rightarrow 42$	$X_{16}, X_{23} \rightarrow 43$	$X_{11}, X_{27} \rightarrow 44$
$X_{16}, X_{25} \rightarrow 45$	$X_{13}, X_{23} \rightarrow 46$	$X_{13}, X_{22} \rightarrow 47$	$X_{18}, X_{26} \rightarrow 48$
$X_{14}, X_{26} \rightarrow 49$	$X_{15}, X_{24} \rightarrow 50$	$X_{17}, X_{23} \rightarrow 51$	$X_{14}, X_{27} \rightarrow 52$
$X_{17}, X_{25} \rightarrow 53$	$X_{12}, X_{23} \rightarrow 54$	$X_{12}, X_{22} \rightarrow 55$	$X_{15}, X_{26} \rightarrow 56$
$X_{16}, X_{21} \rightarrow 57$	$X_{13}, X_{27} \rightarrow 58$	$X_{11}, X_{28} \rightarrow 59$	$X_{16}, X_{24} \rightarrow 60$
$X_{11}, X_{22} \rightarrow 61$	$X_{18}, X_{28} \rightarrow 62$	$X_{18}, X_{25} \rightarrow 63$	$X_{13}, X_{21} \rightarrow 64$

Table 3.3: The proposed mapping for 2-dimensional 8QAM scheme(2)

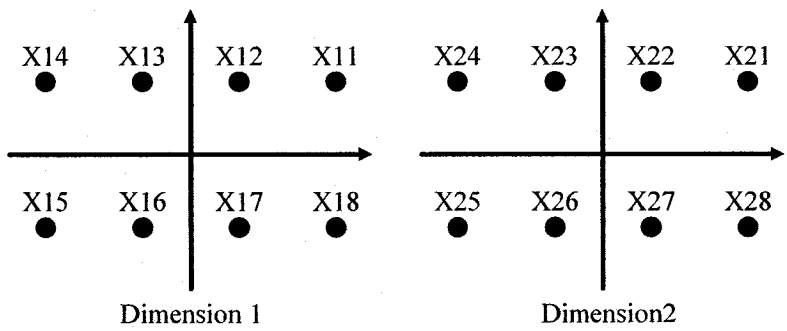

Figure 3.5: 2-dimensional 8QAM constellation scheme(1)

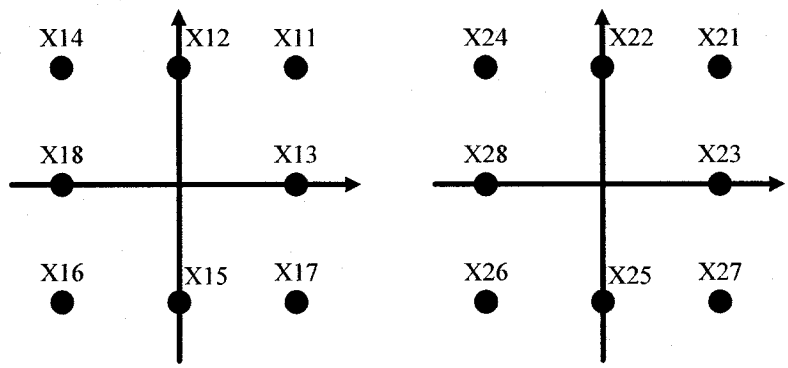

Figure 3.6: 2-dimensional 8QAM constellation scheme(2)

The proposed mapping for 2-dimensional 8PSK is depicted in Fig. 3.7 followed by table 3.4 which shows the index assignments for corresponding constellation.

The proposed mapping for 3-dimensional QPSK is depicted in Fig. 3.8 followed by table 3.5 which shows the index assignments for corresponding constellation.

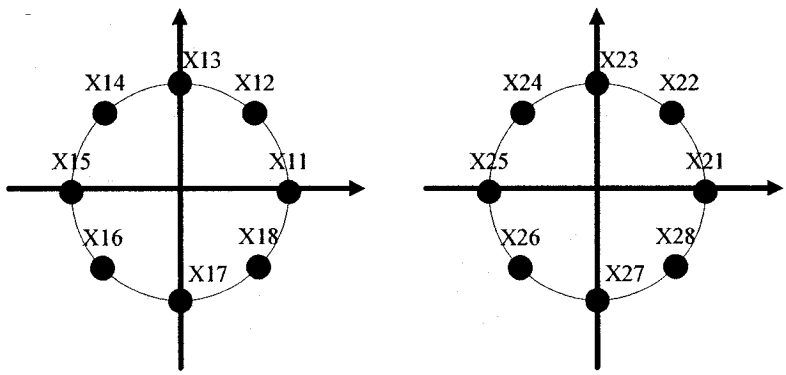

Figure 3.7: 2-dimensional 8PSK constellation scheme

$X_{16}, X_{22} \rightarrow 1$	$X_{12}, X_{26} \rightarrow 2$	$X_{12}, X_{24} \rightarrow 3$	$X_{15}, X_{28} \rightarrow 4$
$X_{12}, X_{21} \rightarrow 5$	$X_{15}, X_{24} \rightarrow 6$	$X_{16}, X_{27} \rightarrow 7$	$X_{11}, X_{22} \rightarrow 8$
$X_{11}, X_{25} \rightarrow 9$	$X_{14}, X_{21} \rightarrow 10$	$X_{15}, X_{21} \rightarrow 11$	$X_{18}, X_{25} \rightarrow 12$
$X_{15}, X_{27} \rightarrow 13$	$X_{11}, X_{24} \rightarrow 14$	$X_{18}, X_{24} \rightarrow 15$	$X_{14}, X_{28} \rightarrow 16$
$X_{14}, X_{25} \rightarrow 17$	$X_{18}, X_{22} \rightarrow 18$	$X_{18}, X_{28} \rightarrow 19$	$X_{14}, X_{24} \rightarrow 20$
$X_{18}, X_{26} \rightarrow 21$	$X_{13}, X_{28} \rightarrow 22$	$X_{14}, X_{23} \rightarrow 23$	$X_{17}, X_{26} \rightarrow 24$
$X_{17}, X_{21} \rightarrow 25$	$X_{15}, X_{25} \rightarrow 26$	$X_{12}, X_{25} \rightarrow 27$	$X_{16}, X_{21} \rightarrow 28$
$X_{13}, X_{23} \rightarrow 29$	$X_{17}, X_{28} \rightarrow 30$	$X_{16}, X_{28} \rightarrow 31$	$X_{13}, X_{24} \rightarrow 32$
$X_{12}, X_{28} \rightarrow 33$	$X_{16}, X_{24} \rightarrow 34$	$X_{16}, X_{23} \rightarrow 35$	$X_{12}, X_{27} \rightarrow 36$
$X_{16}, X_{25} \rightarrow 37$	$X_{11}, X_{28} \rightarrow 38$	$X_{12}, X_{22} \rightarrow 39$	$X_{16}, X_{26} \rightarrow 40$
$X_{15}, X_{23} \rightarrow 41$	$X_{11}, X_{27} \rightarrow 42$	$X_{11}, X_{26} \rightarrow 43$	$X_{15}, X_{22} \rightarrow 44$
$X_{11}, X_{21} \rightarrow 45$	$X_{15}, X_{26} \rightarrow 46$	$X_{14}, X_{27} \rightarrow 47$	$X_{11}, X_{23} \rightarrow 48$
$X_{18}, X_{23} \rightarrow 49$	$X_{13}, X_{26} \rightarrow 50$	$X_{14}, X_{26} \rightarrow 51$	$X_{18}, X_{21} \rightarrow 52$
$X_{13}, X_{21} \rightarrow 53$	$X_{17}, X_{24} \rightarrow 54$	$X_{18}, X_{27} \rightarrow 55$	$X_{14}, X_{22} \rightarrow 56$
$X_{13}, X_{27} \rightarrow 57$	$X_{17}, X_{23} \rightarrow 58$	$X_{17}, X_{22} \rightarrow 59$	$X_{13}, X_{25} \rightarrow 60$
$X_{17}, X_{25} \rightarrow 61$	$X_{13}, X_{22} \rightarrow 62$	$X_{12}, X_{23} \rightarrow 63$	$X_{17}, X_{27} \rightarrow 64$

Table 3.4: The proposed mapping for 2-dimensional 8PSK scheme

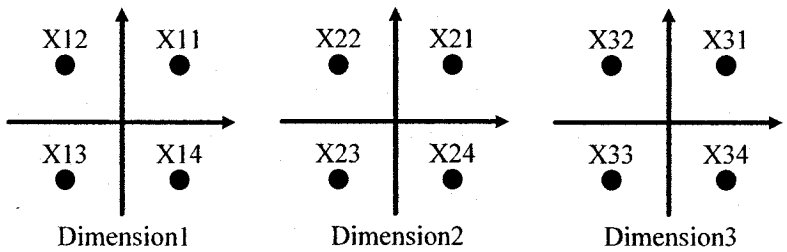

Figure 3.8: 3-dimensional QPSK constellation scheme

$X_{14}, X_{21}, X_{32} \rightarrow 1$	$X_{12}, X_{23}, X_{32} \rightarrow 2$	$X_{13}, X_{23}, X_{31} \rightarrow 3$	$X_{11}, X_{21}, X_{34} \rightarrow 4$
$X_{13}, X_{24}, X_{33} \rightarrow 5$	$X_{14}, X_{22}, X_{31} \rightarrow 6$	$X_{11}, X_{22}, X_{34} \rightarrow 7$	$X_{13}, X_{24}, X_{32} \rightarrow 8$
$X_{13}, X_{22}, X_{34} \rightarrow 9$	$X_{11}, X_{24}, X_{34} \rightarrow 10$	$X_{11}, X_{24}, X_{32} \rightarrow 11$	$X_{13}, X_{22}, X_{32} \rightarrow 12$
$X_{11}, X_{23}, X_{31} \rightarrow 13$	$X_{13}, X_{21}, X_{33} \rightarrow 14$	$X_{13}, X_{22}, X_{33} \rightarrow 15$	$X_{11}, X_{24}, X_{31} \rightarrow 16$
$X_{11}, X_{23}, X_{34} \rightarrow 17$	$X_{13}, X_{21}, X_{31} \rightarrow 18$	$X_{12}, X_{21}, X_{33} \rightarrow 19$	$X_{14}, X_{23}, X_{32} \rightarrow 20$
$X_{12}, X_{22}, X_{31} \rightarrow 21$	$X_{11}, X_{24}, X_{33} \rightarrow 22$	$X_{14}, X_{24}, X_{32} \rightarrow 23$	$X_{12}, X_{22}, X_{34} \rightarrow 24$
$X_{12}, X_{24}, X_{32} \rightarrow 25$	$X_{14}, X_{22}, X_{33} \rightarrow 26$	$X_{14}, X_{22}, X_{34} \rightarrow 27$	$X_{12}, X_{24}, X_{31} \rightarrow 28$
$X_{14}, X_{21}, X_{33} \rightarrow 29$	$X_{12}, X_{23}, X_{31} \rightarrow 30$	$X_{12}, X_{21}, X_{31} \rightarrow 31$	$X_{14}, X_{23}, X_{33} \rightarrow 32$
$X_{12}, X_{23}, X_{34} \rightarrow 33$	$X_{14}, X_{21}, X_{34} \rightarrow 34$	$X_{11}, X_{21}, X_{32} \rightarrow 35$	$X_{12}, X_{23}, X_{33} \rightarrow 36$
$X_{14}, X_{22}, X_{32} \rightarrow 37$	$X_{12}, X_{24}, X_{33} \rightarrow 38$	$X_{13}, X_{24}, X_{34} \rightarrow 39$	$X_{11}, X_{22}, X_{31} \rightarrow 40$
$X_{11}, X_{21}, X_{33} \rightarrow 41$	$X_{13}, X_{23}, X_{32} \rightarrow 42$	$X_{13}, X_{23}, X_{33} \rightarrow 43$	$X_{11}, X_{21}, X_{31} \rightarrow 44$
$X_{13}, X_{24}, X_{31} \rightarrow 45$	$X_{11}, X_{22}, X_{33} \rightarrow 46$	$X_{11}, X_{23}, X_{32} \rightarrow 47$	$X_{13}, X_{21}, X_{34} \rightarrow 48$
$X_{13}, X_{21}, X_{32} \rightarrow 49$	$X_{11}, X_{23}, X_{33} \rightarrow 50$	$X_{13}, X_{23}, X_{34} \rightarrow 51$	$X_{14}, X_{21}, X_{31} \rightarrow 52$
$X_{12}, X_{24}, X_{34} \rightarrow 53$	$X_{13}, X_{22}, X_{31} \rightarrow 54$	$X_{11}, X_{22}, X_{32} \rightarrow 55$	$X_{14}, X_{24}, X_{33} \rightarrow 56$
$X_{14}, X_{23}, X_{31} \rightarrow 57$	$X_{12}, X_{21}, X_{34} \rightarrow 58$	$S_{12}, S_{21}, S_{32} \rightarrow 59$	$S_{14}, S_{23}, S_{34} \rightarrow 60$
$X_{12}, X_{22}, X_{33} \rightarrow 61$	$X_{14}, X_{24}, X_{31} \rightarrow 62$	$S_{14}, S_{24}, S_{34} \rightarrow 63$	$S_{12}, S_{22}, S_{32} \rightarrow 64$

Table 3.5: The proposed mapping for 3-dimensional QPSK scheme

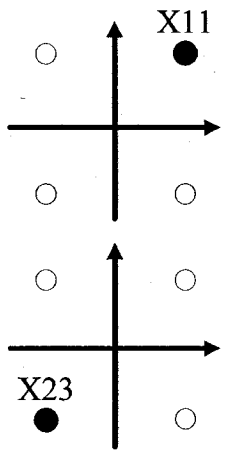

Figure 3.9: $(X_{11}, X_{23} \rightarrow 14)$ illustration for 2-dimensional QPSK

In the above-mentioned tables, each entry $(..., X_{ij}, ... \rightarrow K)$ represents an n-dimensional signal, where i indicates the i-th dimension, j shows the position of the corresponding signal in the conventional constellation and K is a decimal label corresponding to $m \times n$-bit binary number and $(K)_{10} = (m \times n + 1)_2$. Assume an specific signal point $(X_{11}, X_{23} \rightarrow 14)$ chosen from table 3.1 which is a 2-dimensional QPSK constellation. This signal represents "1101" binary bits and depicted in Fig.3.9.

Table 3.6 lists the parameter δ of proposed mappings at $SNR = 10dB$. It is assumed that the average symbol energy is normalized to be one. For a fixed SNR the cost function δ in equation (3.15) can be interpreted as harmonic mean distance with perfect knowledge of other bits $(\tilde{d}_h^2)$. Since $\tilde{d}_h^2$ affects the asymptotic performance of a BICM-ID system, it is expected that a mapping with smaller δ leads to lower asymptotic performance in MIMO-BICM-ID systems. This is confirmed with simulation in Chapter 4. Therefore, in the sense of achieving optimum asymptotic performance in MIMO-BICM-ID systems, the constellation or mapping with smaller δ is required. Considering the table 3.6, 3-dimensional QPSK has the smallest δ

Constellation and Mapping Type	δ
2-dimensional QPSK	8.33e-02
2-dimensional 8QAM(1)	7.47e-02
2-dimensional 8QAM(2)	6.58e-02
2-dimensional 8PSK	6.51e-02
3-dimensional QPSK	4.53e-02

Table 3.6: The parameter δ for the proposed mappings

among the mentioned constellation and mappings.

3.5 Evaluation of Proposed Constellations/Mappings

Constellations and mappings can be evaluated basically in three ways. Mutual information, EXIT charts and distance spectrums are suggested approaches. Using either Mutual Information or EXIT chart is preferred in the sense of visualizing the characteristic of the mapping or constellation. In this section, the proposed constellations and mappings are evaluated based on mutual information.

3.5.1 Study of proposed constellations/mappings by Mutual Information

One of the approaches to evaluate a mapping, is to measure the information about the transmitted signal (X) provided by the received signal (Y) (channel observations). This is expressed in [45]:

$$I(X;Y) = \oint \oint p(X,Y) \cdot \log \frac{p(X,Y)}{p(X) \cdot p(Y)} d_X d_Y \tag{3.16}$$

Consider an M-ary constellation ψ where $M = 2^m$. The channel output $\mathbf{r}$ is described as:

$$\mathbf{r} = \mathbf{H} \cdot \mathbf{s} + \mathbf{n} \tag{3.17}$$

The average symbol-wise mutual information for SISO systems over AWGN channel is defined as:

$$I(s;r) = \frac{1}{M} \sum_{k=1}^{M} \int_{-\infty}^{+\infty} p(r|s_k) \cdot \log_2 \frac{p(r|s_k)}{p(r)} dr \tag{3.18}$$

In the multi-dimensional case where each constellation signal represents $n \times m$ bits, the average mutual information can be expressed as:

$$I(\mathbf{s};\mathbf{r}) = \frac{1}{2^{n\times m}} \sum_{k=1}^{n\times m} \int_{-\infty}^{+\infty} p(\mathbf{H}) \int_{-\infty}^{+\infty} p(\mathbf{r}|\mathbf{s}_k) \cdot \log_2 \frac{p(\mathbf{r}|\mathbf{s}_k)}{p(\mathbf{r})} d\mathbf{r} d\mathbf{H} \tag{3.19}$$

where

$$p(\mathbf{r}) = \frac{1}{2^{n\times m}} \sum_{k=1}^{2^{n\times m}} p(\mathbf{r}|\mathbf{s}_k) \tag{3.20}$$

In the equation (3.19) integration over $\mathbf{r}$ and $\mathbf{H}$ are two-fold integrals. On the other hand, $p(\mathbf{r}|\mathbf{s}_k)$ is easily found from equation (3.17),

$$p(\mathbf{r}|\mathbf{s}_k) = \frac{1}{(2\pi\sigma^2)^N} \cdot \exp\left(-\frac{\|\mathbf{r} - \mathbf{H} \cdot \mathbf{s}_k\|^2}{2\sigma^2}\right) \tag{3.21}$$

where $\delta^2 = \frac{N_o}{2}$ (double-sided noise power spectral density) and N is the number of dimensions. In our system of interest which is a specific case, N is equal to N_t (number of transmitter and receiver antennas). For example consider a 2-dimensional

case where the system uses two transmit and receive antennas over AWGN channel. $p(\mathbf{r}|\mathbf{s}_k)$ can be written as,

$$p(\mathbf{r}|\mathbf{s}_k) = \frac{1}{(\pi N_o)^2} \exp\left(-\frac{|r_1 - x_1|^2 + |r_2 - x_2|^2}{N_o}\right) \tag{3.22}$$

where receive and transmit signals are represented as r_1 and x_1 in dimension 1 and as r_2 and x_2 in dimension 2, respectively.

For the multi-dimensional constellation over fading channels evaluating average mutual information using several multi-dimensional integration is prohibitive. We can estimate this mutual information with a Monte-carlo simulation. Consider transmission over AWGN channel with N_n samples of the noise, we use Monte-Carlo method for simulating the symbol-wise mutual information using the following equation

$$I(\mathbf{s};\mathbf{r}) = \frac{1}{N_n} \sum_{n=1}^{N_n} \log_2 \frac{p(\mathbf{r}_n|\mathbf{s}_n)}{\frac{1}{2^{n\times m}} \sum_{k=1}^{2^{n\times m}} p(\mathbf{r}_n|\mathbf{s}_k)} \tag{3.23}$$

This can be modified for transmission over fading channels. The mutual information using Monte-Carlo simulation with N_H number of samples of channel state, can be described as:

$$I(\mathbf{s};\mathbf{r}) = \frac{1}{N_n N_H} \sum_{h=1}^{N_H} \sum_{n=1}^{N_n} \log_2 \frac{p(\mathbf{r}_n|\mathbf{s}_n, \mathbf{H}_h)}{\frac{1}{2^{n\times m}} \sum_{k=1}^{2^{n\times m}} p(\mathbf{r}_n|\mathbf{s}_k, \mathbf{H}_h)} \tag{3.24}$$

Here we define the bit-wise mutual information. Bit-wise mutual information is a technique to measure the information about the each of the bits in a symbol label by observing the received symbol. This mutual information can be defined in two ways. One is evaluating bit-wise mutual information without any knowledge about other bits I_0. The other one is bit-wise mutual information with perfect knowledge

about other bits I_1. Consider a MIMO communication system and let $[c_1, c_2, ..., c_{n\times m}]$ denote the $n \times m$ bits mapped to one symbol in the constellation ϕ. The average bit-wise mutual information without any knowledge about other bits can be expressed as:

$$I_0 = \frac{1}{n \times m} \sum_{k=1}^{n\times m} I(c_k; \mathbf{r}) \tag{3.25}$$

where

$$I(c_k; \mathbf{r}) = \frac{1}{2} \sum_{b=0}^{1} I(c_k = b; \mathbf{r}) \tag{3.26}$$

and $I(c_k = b; \mathbf{r})$ is calculated as:

$$\begin{aligned} I(c_k = b; \mathbf{r}) = & \int_{-\infty}^{+\infty} p(\mathbf{H}) \int_{-\infty}^{+\infty} \left(\frac{1}{2^{n\times(m-1)}} \sum_{\mathbf{s}_j \in \phi_b^k} p(\mathbf{r}|\mathbf{s}_j) \right) \\ & \times \log_2 \frac{\left(\frac{1}{2^{n\times(m-1)}} \sum_{\mathbf{s}_j \in \phi_b^k} p(\mathbf{r}|\mathbf{s}_j) \right)}{\frac{1}{2} \cdot \frac{1}{2^{n\times(m-1)}} \left[\sum_{\mathbf{s}_j \in \phi_b^k} p(\mathbf{r}|\mathbf{s}_j) + \sum_{\mathbf{s}_j \in \phi_b^i} p(\mathbf{r}|\mathbf{s}_j) \right]} d\mathbf{r} d\mathbf{H} \end{aligned} \tag{3.27}$$

$$I(c_k = b; \mathbf{r}) = \frac{1}{2^{n\times(m-1)}} \sum_{\mathbf{s}_j \in \phi_b^k} \int_{-\infty}^{+\infty} p(\mathbf{H}) \int_{-\infty}^{+\infty} p(\mathbf{r}|\mathbf{s}_j) \cdot \log_2 \frac{2 \cdot \sum_{\mathbf{s}_j \in \phi_b^k} p(\mathbf{r}|\mathbf{s}_j)}{\sum_{j=1}^{2^{n\times m}} p(\mathbf{r}|\mathbf{s}_j)} d\mathbf{r} d\mathbf{H} \tag{3.28}$$

In equation (3.27), $\mathbf{s}_j \in \phi_b^k$ denotes the symbols whose labels have the value $b \in [0, 1]$ in their k-th position. For the AWGN channel, the integration over the probability density function p($\mathbf{H}$) of the channel state matrix in equation (3.34), can be omitted. As it has been mentioned, evaluating this mutual information over

fading channels and multi-dimensional constellations, involves with several two-fold integrations. Consider transmission over fading channel with N_n samples of the noise, we use Monte-Carlo method for simulating the average mutual information without knowledge about other bits, using the following equation

$$I_0 = \frac{1}{N_n} \sum_{n=1}^{N_n} \log_2 \frac{2 \cdot \sum_{\mathbf{s}_j \in \phi_b^k} p(\mathbf{r}_n | \mathbf{s}_j, \mathbf{H})}{\sum_{j=1}^{2^{n \times m}} p(\mathbf{r}_n | \mathbf{s}_j, \mathbf{H})} \tag{3.29}$$

In equation (3.29) $\mathbf{s}_j \in \phi_b^k$ denotes symbols whose labels have the value of b in their k-th position ($b = \mu^{-1}(\mathbf{s}_n), k$). b gets the values of either "0" or "1" depending on the k-th position of $\mathbf{s}_n$'s label ($\mathbf{r}_n = \mathbf{H} \cdot \mathbf{s}_n + \mathbf{n}_n$). In calculating I_0, if the channel state is unknown in the receiver, averaging over samples of $\mathbf{H}$ is inevitable.

I_1 is the average bit-wise mutual information with perfect knowledge about the $n \times m - 1$ other bits. The expression for I_1 can be obtained as follows.

$$I_1 = \frac{1}{n \times m} \sum_{k=1}^{n \times m} I(c_k; \mathbf{r} | \text{all other } n \times (m-1) \text{ bits are known}) \tag{3.30}$$

Let $[c_1, c_2, ..., c_{n \times m}]$ denote the $n \times m$ bits mapped to one symbol in constellation ϕ. We define:

$$\underline{\mathbf{C_k}} = [c_1, c_2, ..., c_{k-1}, c_{k+1}, ..., c_{n \times m}] \tag{3.31}$$

and therefore (3.30)can be rewritten as:,

$$I_1 = \frac{1}{n \times m} \sum_{k=1}^{n \times m} I(c_k; \mathbf{r} | \underline{\mathbf{C_k}}). \tag{3.32}$$

$I(c_k; \mathbf{r} | \underline{\mathbf{C_k}})$ can be expressed as:

$$I(c_k;\mathbf{r}|\underline{\mathbf{C_k}}) = \frac{1}{2^{n\times m}}\sum_{b=0}^{1}\sum_{\forall \mathbf{c}_k} I(c_k = b;\mathbf{r}|\underline{\mathbf{C_k}} = \mathbf{c}_k) \tag{3.33}$$

where $\mathbf{c}_k = [b_1, b_2, ..., b_{k-1}, b_{k+1}, b_{n\times m}]$ and b_j gets the values of either 0 or 1. Regarding the mentioned assumptions we evaluate $I(c_k = b;\mathbf{r}|\underline{\mathbf{C_k}} = \mathbf{c}_k)$ by numerical integration:

$$\begin{aligned} I(c_k = b;\mathbf{r}|\underline{\mathbf{C_k}} = \mathbf{c}_k) = \int_{-\infty}^{+\infty} p(\mathbf{H}) \int_{-\infty}^{+\infty} p(\mathbf{r}|c_k = b, \underline{\mathbf{C_k}} = \mathbf{c}_k) \\ \cdot \log_2 \frac{2\cdot p(\mathbf{r}|c_k = b, \underline{\mathbf{C_k}} = \mathbf{c}_k)}{p(\mathbf{r}|c_k = 0, \underline{\mathbf{C_k}} = \mathbf{c}_k) + p(\mathbf{r}|c_k = 1, \underline{\mathbf{C_k}} = \mathbf{c}_k)} d\mathbf{H}d\mathbf{r} \end{aligned} \tag{3.34}$$

with

$$p(\mathbf{r}|c_k = b, \underline{\mathbf{C_k}} = \mathbf{c}_k) = p(\mathbf{r}|\mathbf{s}_j), \qquad \mathbf{s}_j = \mu(c_1, c_2, ..., c_{k-1}, b, c_{k+1}, ..., c_{n\times m}) \tag{3.35}$$

where $\mu(\cdot)$ is the mapping scheme. $p(\mathbf{r}|\mathbf{s}_j)$ is defined in equation (3.21). It is explicit that in calculation of $I(c_k = b;\mathbf{r}|\underline{\mathbf{C_k}} = \mathbf{c}_k)$ we deal only with two symbols, chosen from constellation ϕ. These symbols differ only in their k-th position. For the AWGN channels, the integration over the probability density function p($\mathbf{H}$) of the channel state matrix in equation (3.34), can be omitted. For the multi-dimensional transmission over fading channel, calculating the average mutual information in equation (3.34) is involved with several multi-dimensional integration. As mentioned previously, we use Monte-Carlo method for simulating the mutual information with perfect CSI using

$$I_1 = \frac{1}{N_n}\sum_{n=1}^{N_n} \frac{2\cdot p(\mathbf{r}_n|\mathbf{s}_n, \mathbf{H})}{p(\mathbf{r}_n|\mathbf{s}_n^0, \mathbf{H}) + p(\mathbf{r}_n|\mathbf{s}_n^1, \mathbf{H})}. \tag{3.36}$$

In equation (3.36), N_n is the number of samples of noise and $\mathbf{r}_n = \mathbf{H}\cdot\mathbf{s}_n + \mathbf{n}_n$.

It is clear that $\mathbf{s}_n^0$ and $\mathbf{s}_n^1$ is chosen from the signal constellation ϕ considering $\mathbf{s}_n$. $\mathbf{s}_n^0$ has the same label as $\mathbf{s}_n$ with "0" in its k-th position. It is the same for $\mathbf{s}_n^1$ except its k-th position gets the value of "1".In other words, let $[c_1, ..., c_{n\times m}] = \mu^{-1}(\mathbf{s}_n)$ then $\mathbf{s}_n^0 = \mu(c_1, ..., c_{k-1}, 0, c_{k+1}, ..., c_{n\times m})$ and $\mathbf{s}_n^1 = \mu(c_1, ..., c_{k-1}, 1, c_{k+1}, ..., c_{n\times m})$. There is no doubt that at a time, $\mathbf{s}_n$ will be either $\mathbf{s}_n^0$ or $\mathbf{s}_n^1$. In calculating I_1, if the channel state is unknown in the receiver, averaging over samples of $\mathbf{H}$ is inevitable.

3.5.2 Characterizing the proposed constellation and mappings using mutual information

In this section based on mutual information discussed in the previous section we evaluate the proposed constellation and mappings.

As it has been mentioned, in calculation of the average bit-wise mutual information I_0, it is assumed that there is no information about the other bits. Hence I_0 is an important parameter for the first iteration of systems employing BICM-ID where no information is available to feedback from the decoder. So usually I_0 is more important for BICM systems. If the iterations between the channel decoder and the demodulator start working, then more and more reliable information about other bits in one symbol is delivered to the demodulator [46]. Therefore I_0 is not important any more. Eventually, if a perfect information about all other bits is available at the demodulator, the average mutual information with perfect knowledge about the other bits (I_1) is dominant.

The sum of bit-wise mutual information, for a fixed constellation, is always a constant value (I), independent of the applied mapping [46]. Therefore, there is a trade-off between the bit-wise mutual information. It has been found that, for a

constant constellation, usually a mapping with maximum I_1 induces minimum I_0 and vice versa [27][29]. To have a good performance with no iteration, a mapping should be chosen which maximizes I_0. On the other hand, a mapping with larger I_0 and consequently smaller mutual information with a priori knowledge (I_1), can not gain the error performance of the system through the iterations. Gray mapping is a good sample of such a mapping. Also it has been found that iterative process cannot improve the error performance of a system utilizing a mapping with large I_1 and very small I_0 because of early crossing of the transfer function [47], which would cause the iterative process to stop early[29]. A compromise solution is to find a mapping with big enough I_0 to make the iterations work, while maximizing I_1 to achieve good performance after number of iterations. According to the design criteria defined in the previous sections, we expect to improve the mutual information while there is a perfect (reliable enough) information about the other bits. Although I_0 has not been considered in designing the criteria, result of simulations show that still we get big enough I_0 while I_1 is maximized.

According to the definition in previous section, the mutual information depends on the specific Signal to Noise Ratio (SNR) of the system of interest. Thus to compare mutual information of different mappings, the SNR range should be fixed.

Results of simulations regarding Mutual information of the proposed constellation/mappings are illustrated as follows. First of all the comparison between the symbol-wise mutual information of the proposed constellation/mappings in tables 3.1-3.5, is presented in Fig. 3.10. In comparison between two different constellations, although the symbol-wise mutual information is independent of the applied mapping, the one with the higher symbol-wise mutual information is preferred. Since choosing

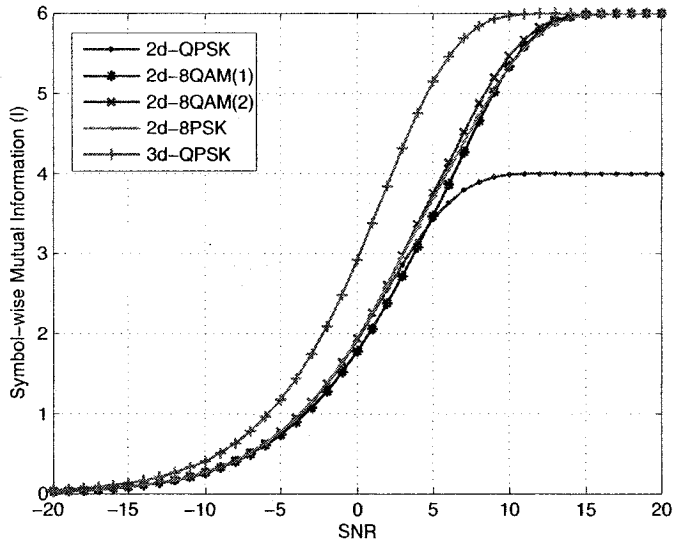

Figure 3.10: Symbol-wise mutual information for different multi-dimensional constellation

the constellation with higher symbol-wise mutual information gives the pliability to design the desired values of the bit-wise mutual information. Therefore, 3-dimensional QPSK is preferred to 2-dimensional 8QAM or 8PSK, considering Fig. 3.10.

Figs. 3.11-3.20 show the simulation result for the average bit-wise mutual information versus symbol-wise mutual information for proposed constellations/mappings. These illustrations are useful to compare two mapping schemes for a fixed constellation. According to our design criteria and the discussion in the previous paragraph, it is required that the proposed mapping maximizes I_1 while I_0 is still reasonable. Figs. 3.11-3.20 present that conventional mapping schemes have almost the same I_0 and I_1. For each constellation and mapping two graphs are depicted, one for the average bit-wise mutual information without perfect a priori information (I_0) and another for the average bit-wise mutual information with perfect a priori information (I_1). In

each figure a comparison between conventional mapping and proposed one is made. It is shown that all proposed mappings maximize I_1 while I_0 is still big enough to make iterations work. There is always a trade-off between I_1 and I_0, maximizing I_1 results in minimizing I_0.

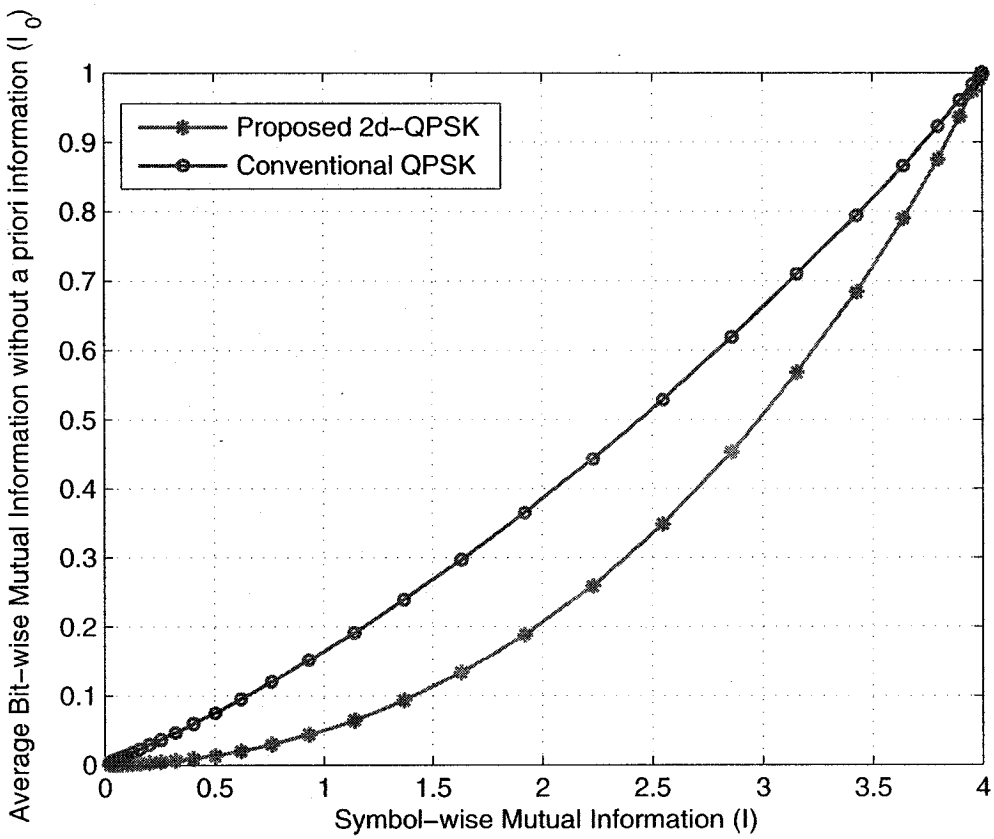

Figure 3.11: The average bit-wise mutual information without a priori information (I_0) versus symbol-wise mutual information (I) for 2-dimensional QPSK

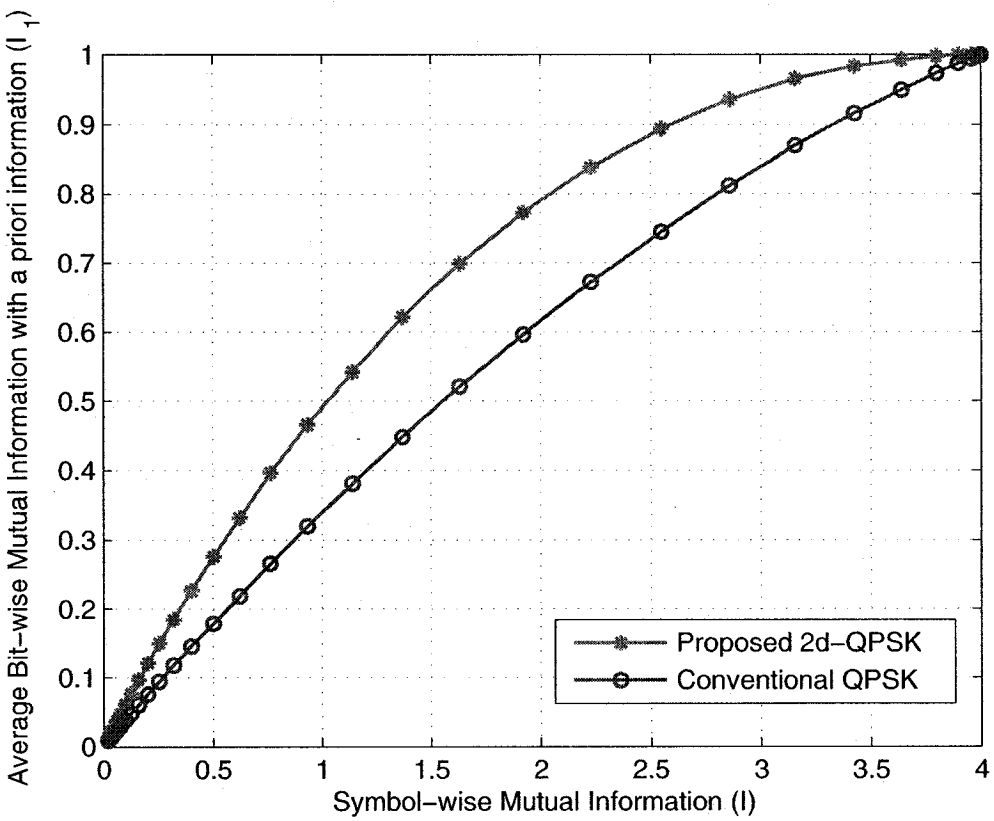

Figure 3.12: The average bit-wise mutual information with perfect a priori information (I_1) versus symbol-wise mutual information (I) for 2-dimensional QPSK

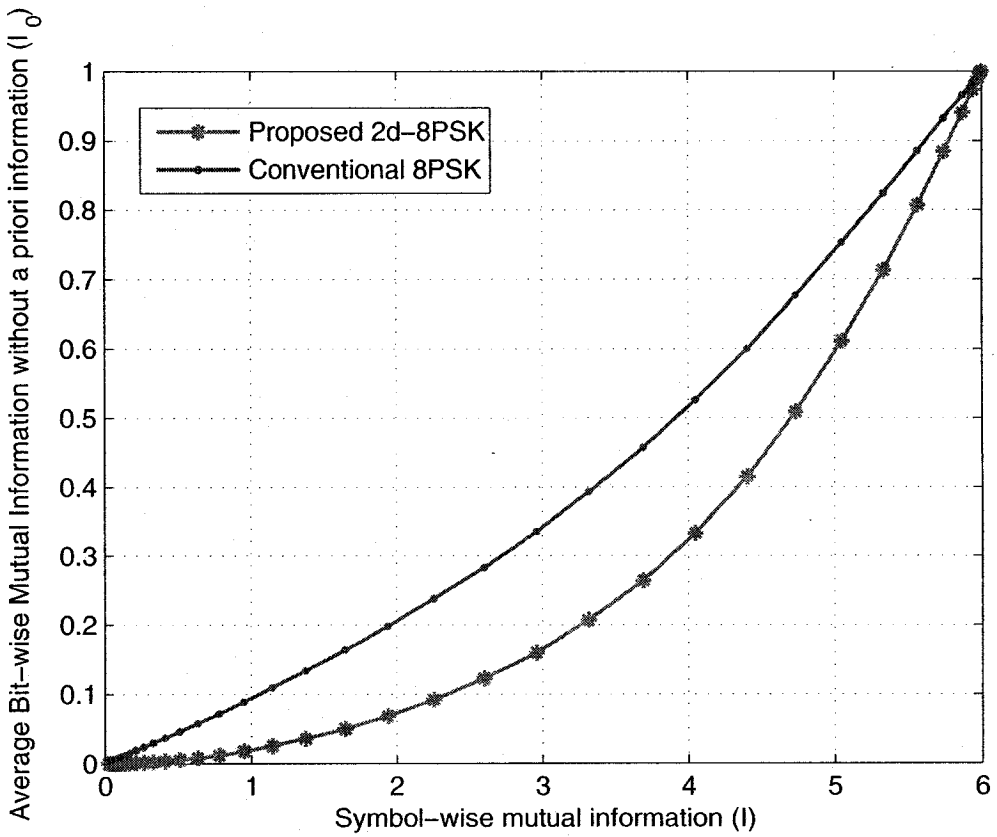

Figure 3.13: The average bit-wise mutual information without perfect a priori information (I_0) versus symbol-wise mutual information (I) for 2-dimensional 8PSK

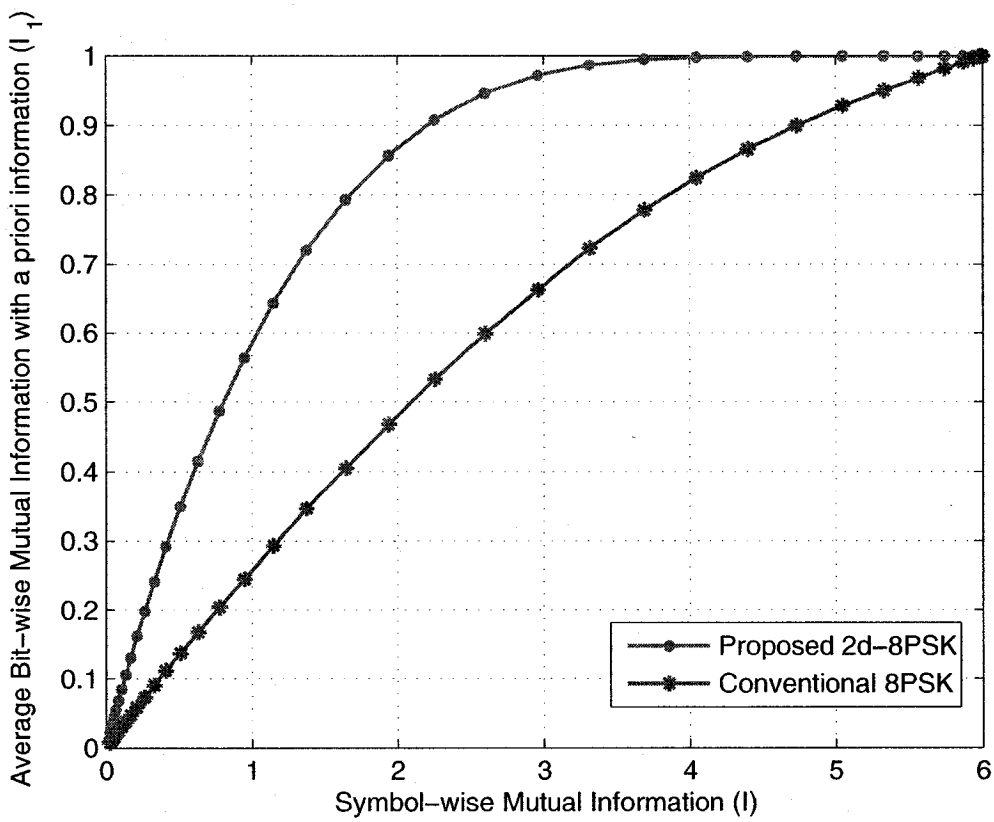

Figure 3.14: The average bit-wise mutual information with perfect a priori information (I_1) versus symbol-wise mutual information (I) for 2-dimensional 8PSK

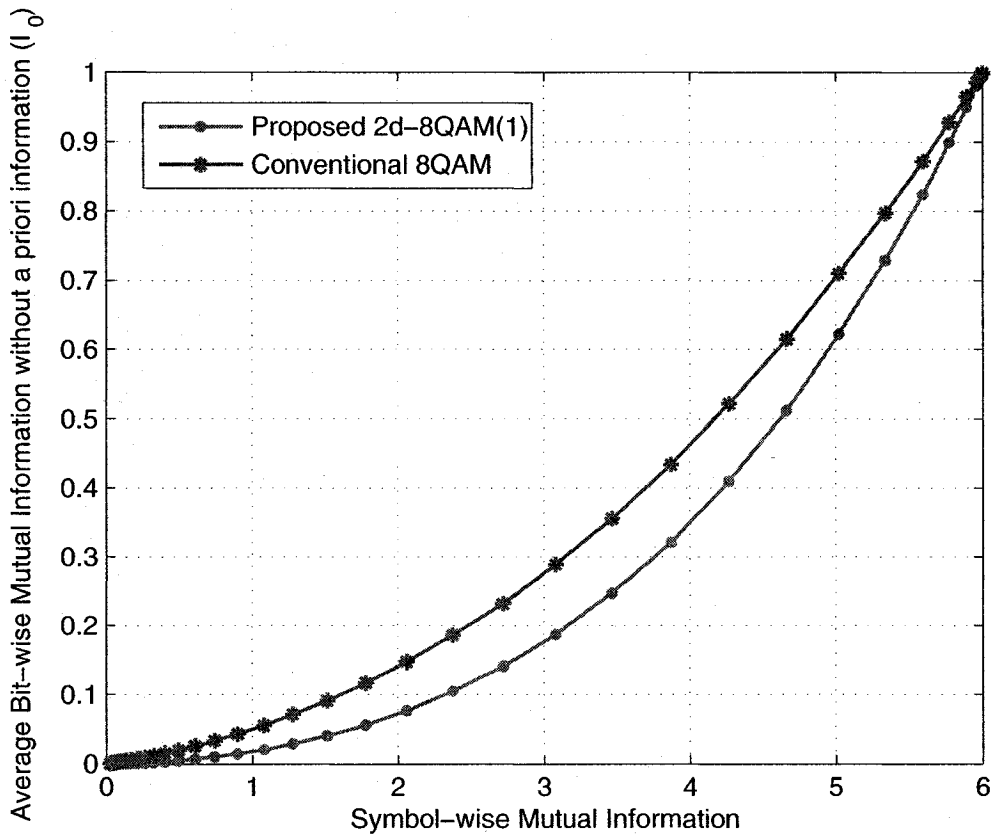

Figure 3.15: The average bit-wise mutual information without perfect a priori information (I_0) versus symbol-wise mutual information (I) for 2-dimensional 8QAM(1)

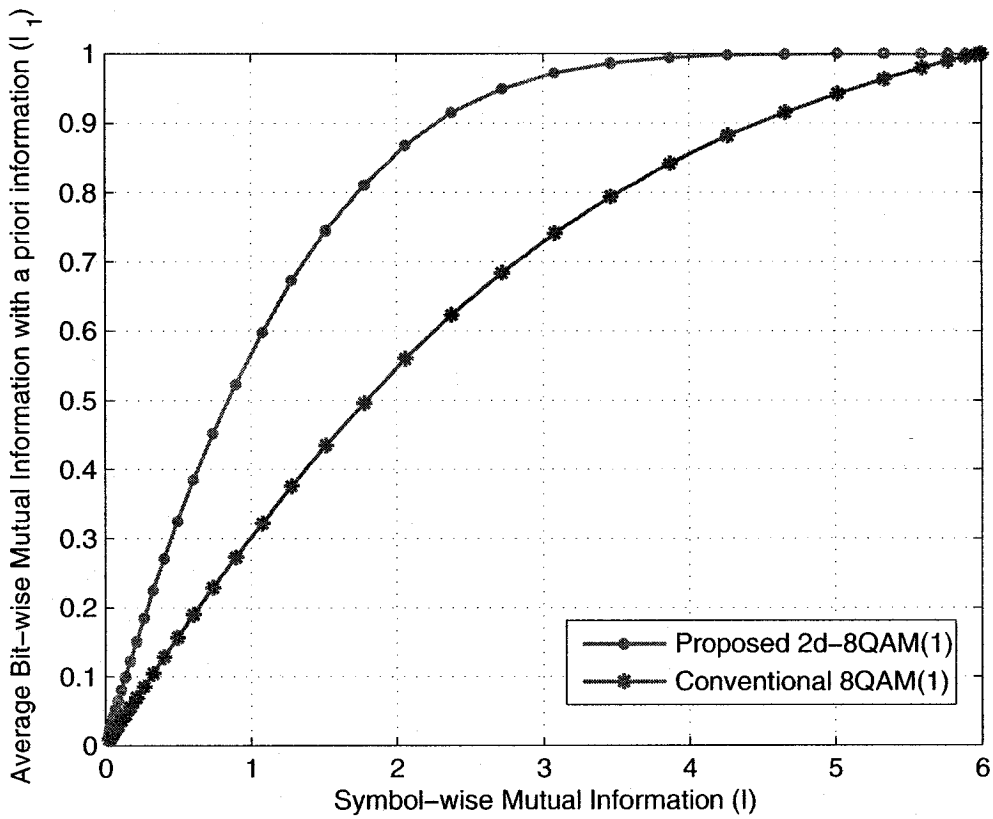

Figure 3.16: The average bit-wise mutual information with perfect a priori information (I_1) versus symbol-wise mutual information (I) for 2-dimensional 8QAM(1)

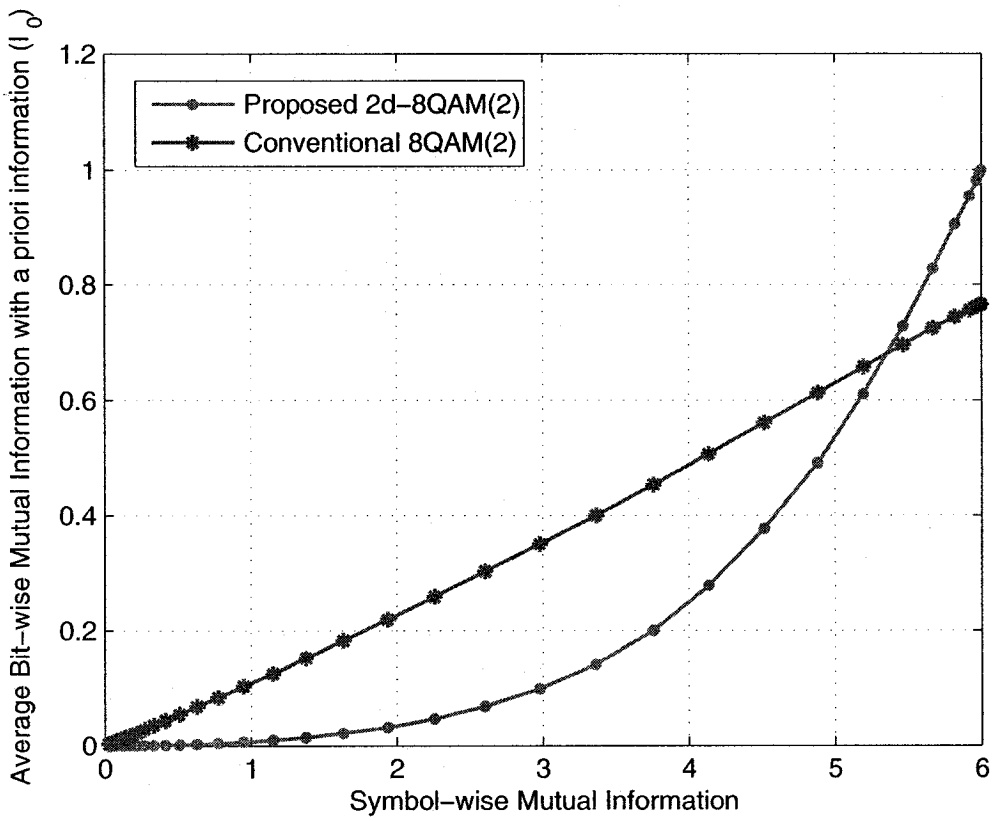

Figure 3.17: The average bit-wise mutual information without perfect a priori information (I_0) versus symbol-wise mutual information (I) for 2-dimensional 8QAM(2)

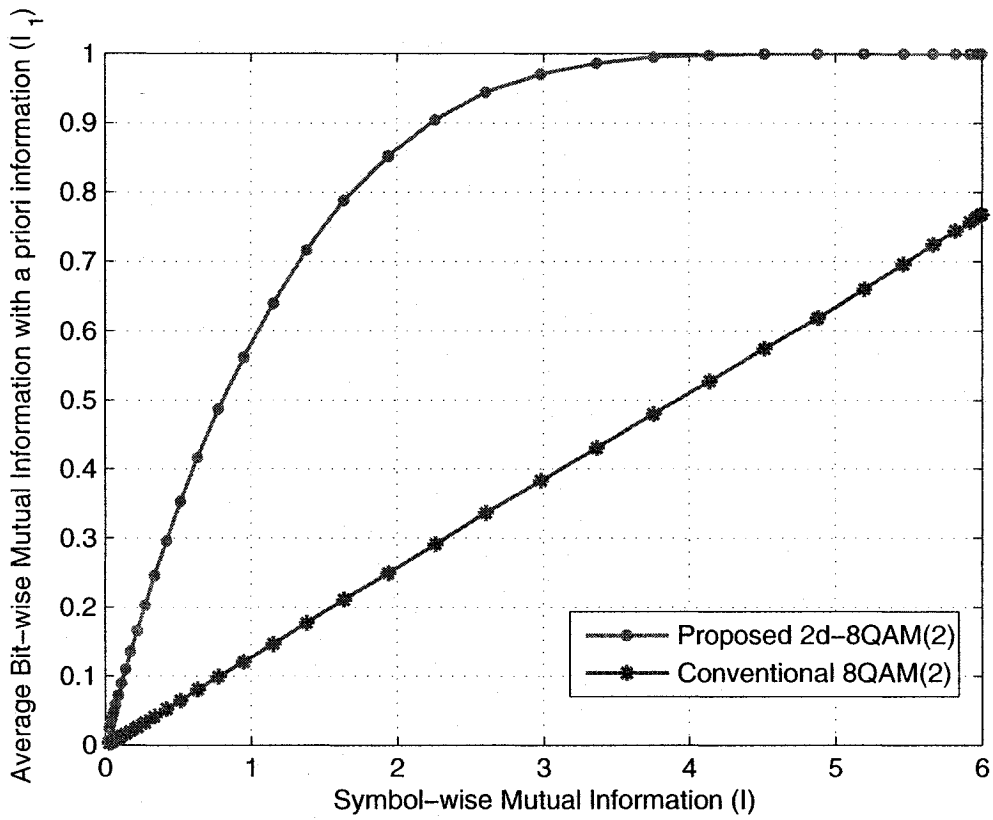

Figure 3.18: The average bit-wise mutual information with perfect a priori information (I_1) versus symbol-wise mutual information (I) for 2-dimensional 8QAM(2)

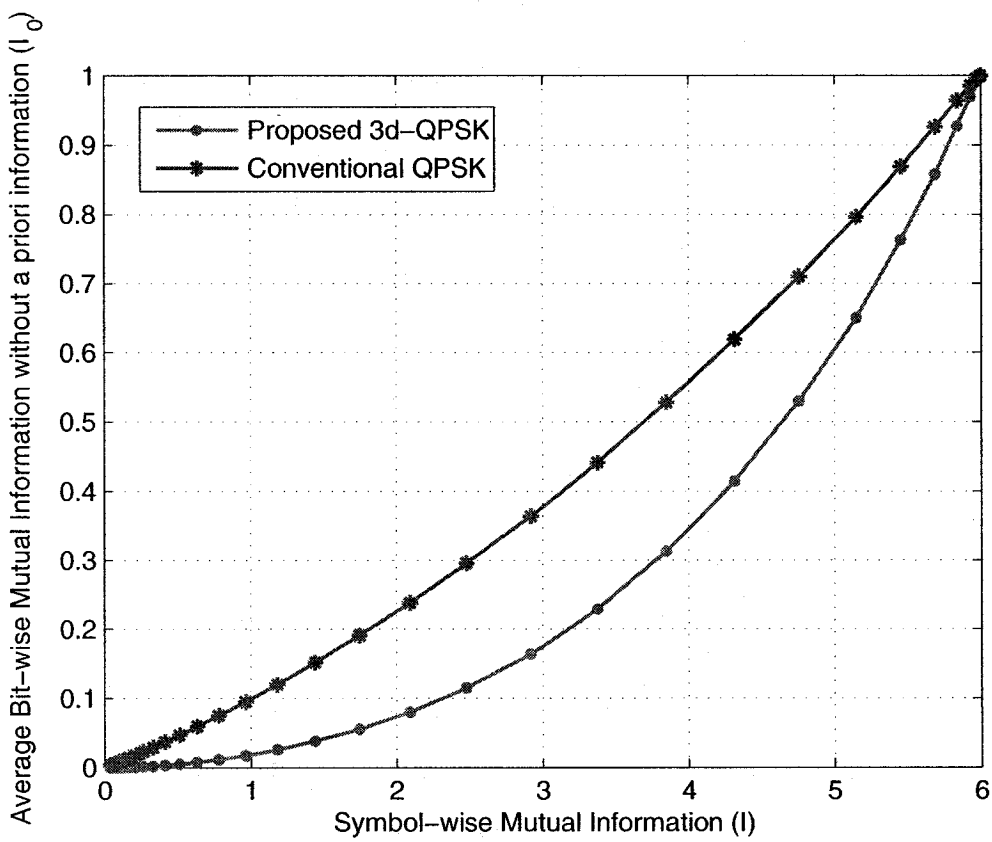

Figure 3.19: The average bit-wise mutual information without perfect a priori information (I_0) versus symbol-wise mutual information (I) for 3-dimensional QPSK

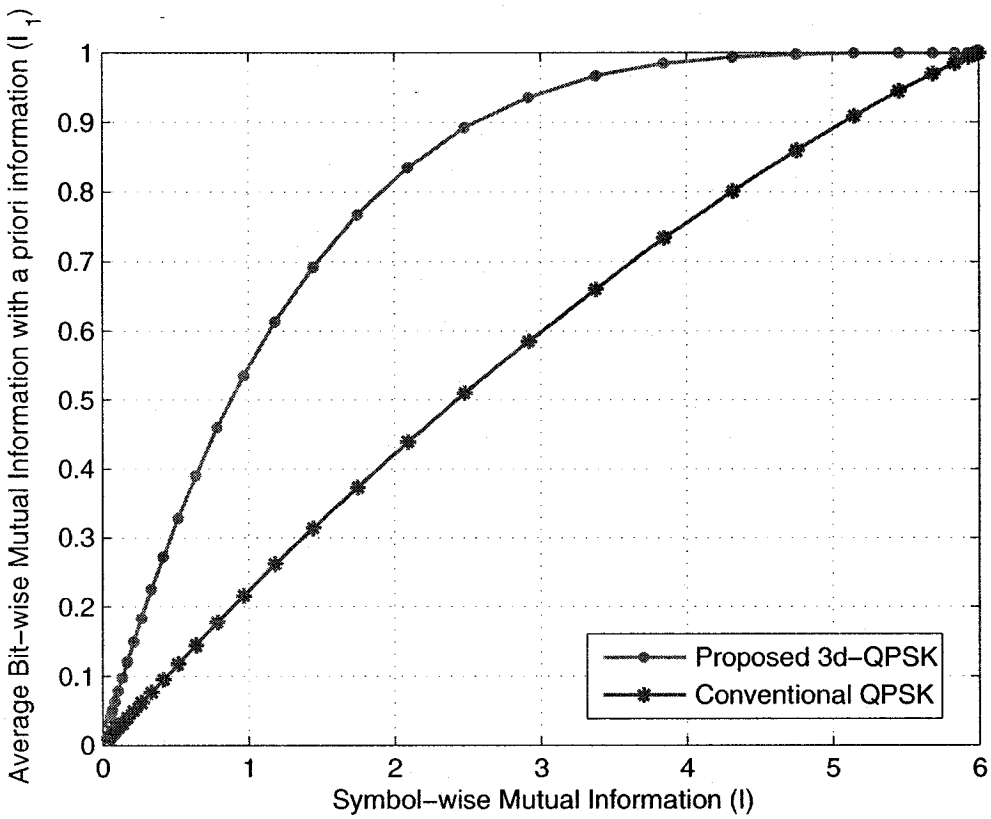

Figure 3.20: The average bit-wise mutual information with perfect a priori information (I_1) versus symbol-wise mutual information (I) for 3-dimensional QPSK

3.6 Summary

In this chapter, it is mentioned that signal mapping has a critical influence on the error performance of communication systems performing based on BICM-ID concept. Therefore, a system model for MIMO-BICM-ID transmitter based on multi-dimensional mapping has been proposed. This new constellation is based on mapping information bits to the parallel symbols and sending them over N_t transmitter antennas.

An upper bound for pairwise error probability is derived and based on PEP, a cost function is defined. Binary Switching Algorithm is modified to be used in choosing optimum mappings. A few multi-dimensional mappings are found and introduced based on the cost function by using computer search utilizing BSA. Two kinds of bit-wise mutual information according to a priori information are defined. A model for simulation, to be used in Monte-carlo method is proposed. Finally, proposed mappings are evaluated based on mutual information. Simulations of bit-wise mutual information for the proposed constellations/mappings are presented. Regarding bit-wise mutual information comparison has been made between the conventional mapping schemes and proposed schemes.

Chapter 4

MIMO-BICM-ID Receiver Based on Sphere Decoder

In this chapter, the focus is to design a receiver for the transmitter proposed in Fig. 3.1. This receiver is designed considering the receiver introduced in [31]. Such a design will resolve the diversity problem introduced by spatial multiplexing. For simplicity, our simulations consider only examples where the number of transmit and receive antennas are equal. Simulation results show that we can achieve good performance using a simple bit-interleaver, simple convolutional code and a simple V-Blast. The detector/demapper is designed according to the multi-dimensional constellation proposed in Chapter 3. The modified detector/demapper works based on List Sphere Decoder.

4.1 System Model

Recently, the turbo principle, originally proposed for decoding parallel concatenated turbo codes [2], has found applications in various communications systems. In [48][49], it has been shown that the performance of demapping a multilevel modulated signal (e.g. QSPK or 16-QAM) can be improved by using iterative demapping and decoding. The concept of using iterative detection and decoding has been extended to MIMO systems in [31]. In these communication systems, transmitters are modelled as a serial concatenation of outer code and an inner linear MIMO modulation. This method is the most promising technique for high data rate applications. The system combines powerful and well-known conventional binary codes with simple spatial multiplexing schemes on the basis of working in an iterative fashion [31]. In this thesis, this system which is called MIMO-BICM-ID is considered.

Fig. 4.1 illustrates the MIMO-BICM-ID scheme. In Fig. 4.1, at the transmitter information bits $\mathbf{b}$ are first encoded then randomly permuted by passing through a bit interleaver. Coded and interleaved bits are grouped into blocks with $n \times m$ bits ($n = N_t$ and $m = \log_2 M$ where M is the constellation size of conventional modulation scheme). Each block is mapped to a multi-dimensional signal according to the mapping function $\mu(\cdot)$ ($\mathbf{s}_k = \mu(\mathbf{c}_k)$). The mapping scheme has been proposed and discussed in the Chapter 3. The multi-dimensional signal is sent simultaneously over N_t transmitter antennas. It should be mentioned that for multi-user systems, each user has its own channel encoder, interleaver and mapper. The symbol vector corresponding to one block of coded and interleaved bits is denoted by $\mathbf{s}_k = \{x_{1,k}, x_{2,k}, ..., x_{n,k}\}^T$ where n is the number of dimensions and $n = N_t$. x_i is one of the conventional constellation points (i.e. QPSK constellation or 8QAM constellation). Despite the

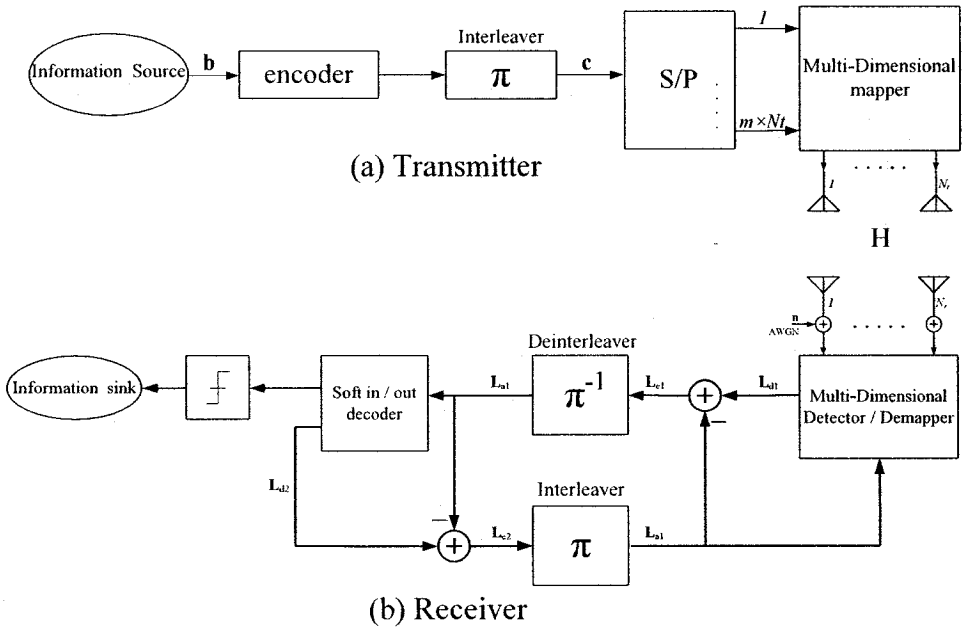

Figure 4.1: The MIMO-BICM-ID scheme

conventional MIMO system, these transmitted symbols are not independent. It is assumed that the average symbol energy is equal to 1, i.e. $E[\|\mathbf{x}_i\|^2] = \frac{E_s}{N_t}$. The N_r-dimensional received signal vector $\mathbf{r_k} = \{r_{1,k}, r_{2,k}, ..., r_{N_r,k}\}^T$ at the symbol-sampled instant k can be modelled as

$$\mathbf{r}_k = \mathbf{H}_k \mathbf{s}_k + \mathbf{n}_k \tag{4.1}$$

where $\mathbf{s}_k$ denotes the N_t-dimensional transmitted symbol vector and $\mathbf{H}_k$ is the MIMO channel associated with $\mathbf{s}_k$. The channel matrix $\mathbf{H}$ is an $N_r \times N_t$ complex matrix whose element h_{ij} is the channel gain from the i-th transmit antenna to the j-th receive antenna. h_{ij} is assumed to be independent and identically distributed (*i.i.d.*) complex Gaussian random variable with zero mean and unit variance. $\mathbf{n}_k =$

$\{n_{1,k}, n_{2,k}, ..., n_{N_r,k}\}^T$ is N_r-dimensional Additive White Gaussian Noise vector. The entries of $\mathbf{n}$ assumed to be $i.i.d$ complex Gaussian random variables with zero mean and variance of $\sigma^2 = \frac{N_o}{2}$ (double sided noise spectral density).

At the receiver side, for optimally decoding $\mathbf{c}_1, \mathbf{c}_2, ...$ blocks, the joint detector and decoder should calculate the likelihood of each bit given all received symbols $\mathbf{r}_1, \mathbf{r}_2, ...$. This is impractical due to computational complexity . The joint iterative detection and decoding based on the turbo principle can be applied to achieve near-optimal solution while complexity is reasonable [31].

4.2 Iterative Receiver

The iterative receiver of Fig. 4.1, utilizes two soft-input soft-output (SISO) blocks, the inner demodulator/demapper and the outer decoder. Although, separate demodulator/demapper and channel decoder are individually optimal, the receiver will be sub-optimal due to this separation. Information between the detector and decoder is exchanged in an iterative fashion until the convergence is achieved as illustrated in Fig. 4.1(b). The optimal algorithm for the outer SISO decoder is derived by Bahl *et al* in [50] which is known as BCJR decoder algorithm. Therefore, in this thesis we focus on the inner detector/demapper.

Assume one channel use of equation (4.1). The *a posteriori*(APP) LLR (Log-Likelihood Ratio) of the i-th bit in the label of multi-dimensional signal input $\mathbf{s}$ using the corresponding channel observation $\mathbf{r}$ can be written as

$$
\begin{aligned}
L_d(c_i|\mathbf{r}) &= \ln \frac{P(c_i = 1|\ \mathbf{r})}{P(c_i = 0|\ \mathbf{r})} \\
&= \ln \left(\frac{P(\mathbf{r}|c_i = 1)}{P(\mathbf{r}|c_i = 0)} \cdot \frac{P(c_i = 1)}{P(c_i = 0)} \right)
\end{aligned}
\tag{4.2}
$$

and $La(c_i) = \frac{P(c_i=1)}{P(c_i=0)}$ is *a priori* information regarding c_j.

According to the proposed transmitter in Chapter 3, encoded bits are scrambled using the bit-interleaver and then sent to the multi-dimensional mapper. Interleaver separates neighbor coded bits as far as possible. Therefore, comprising bits of the block $\mathbf{c} = \mu^{-1}(\mathbf{s})$, are statistically independent of each other. The demodulator/demapper produces the APP LLR of the i-th bit in the block $\mathbf{c}$ based on the *a priori* LLRs, $\mathbf{L}_{a1} = [L_{a1,c_1}, L_{a1,c_2}, ..., L_{a1,c_{N_t \times m}}]$ and corresponding channel observation $\mathbf{r}$. These *a priori* LLRs are sent by the SISO outer decoder for block $\mathbf{c}$ at the previous iteration. The APP LLRs of the i-th bit of the block $\mathbf{c}$ can be written as,

$$
L_{d1,c_i} = L_{e1,c_i} + L_{a1,c_i} \tag{4.3}
$$

$$
L_{d1,c_i} = \underbrace{\ln \frac{P(c_i = 1|\mathbf{y}, \mathbf{L}_{a1}^{c_i})}{P(c_i = 0|\mathbf{y}, \mathbf{L}_{a1}^{c_i})}}_{L_{e1,c_i}} + L_{a1,c_i} \tag{4.4}
$$

where $\mathbf{L}_{a1}^{c_i} = [L_{a1,c_1}, L_{a1,c_2}, ..., L_{a1,c_{i-1}}, L_{a1,c_{i+1}}, ..., L_{a1,c_{N_t \times m}}]$ and variables with subscript "1" are associated with inner detector.

Employing Bayes' theorem and using the independency of $c_1, ..., c_{N_t \times m}$, the *extrinsic* LLRs which are produced by the demodulator/demapper, can be written as

$$
L_{e1,c_i} = \ln \frac{\sum_{\mathbf{c} \in \mathcal{C}_{i,1}} P(\mathbf{r}|\mathbf{c}) \cdot \exp \sum_{k \in \Gamma_{k,\mathbf{c}}} L_{a1}(c_k)}{\sum_{\mathbf{c} \in \mathcal{C}_{i,0}} P(\mathbf{r}|\mathbf{c}) \cdot \exp \sum_{k \in \Gamma_{k,\mathbf{c}}} L_{a1}(c_k)} \tag{4.5}
$$

where $\mathcal{C}_{i,1}$ is the set of $2^{N_t \times m}$ bit vectors $\mathbf{c}$ having $c_i = 1$. In other words, $\mathcal{C}_{i,1} = \{\mathbf{c}|c_i = 1\}$ and $\mathcal{C}_{i,0} = \{\mathbf{c}|c_i = 0\}$. $\Gamma_{k,\mathbf{c}}$ is the set of indices k with $\Gamma_{k,\mathbf{c}} = \{1 \leq k \preceq N_t \times m \quad \text{and} \quad k \neq i\}$.

Instead of using *a priori* LLRs in equation (4.5), we can use the *a priori* probability information provided by BCJR decoder as follows

$$L_{e1,c_i} = \ln \frac{\sum_{\mathbf{c}\in\mathcal{C}_{i,1}} P(\mathbf{r}|\mathbf{c}) \cdot \prod_{l=1,l\neq k}^{N_t\times m} P(c_k)}{\sum_{\mathbf{c}\in\mathcal{C}_{i,0}} P(\mathbf{r}|\mathbf{c}) \cdot \prod_{l=1,l\neq k}^{N_t\times m} P(c_k)} \tag{4.6}$$

where $P(c_k)$ is the probability provided by BCJR decoder.

An essential part for computing LLR values for demodulator/demapper using equations (4.5) or (4.6) is the likelihood function $p(\mathbf{r}|\mathbf{c})$. It should be noted that our mapping scheme is multi-dimensional as described in Chapter 3. Therefore $p(\mathbf{r}|\mathbf{c})$ can be found from equation (4.1) as,

$$P(\mathbf{r}|\ \mathbf{s} = \mu(\mathbf{c})) = \frac{1}{(2\pi\sigma^2)^{N_t}} \cdot \exp\left(-\frac{\|\mathbf{r} - \mathbf{Hs}\|^2}{2\sigma^2}\right) \tag{4.7}$$

where $\sigma^2 = \frac{N_o}{2}$(double-sided noise power spectral density).

Using equation (4.7), we can rewrite the equation (4.6) as follows

$$L_{e1,c_i} = \ln \frac{\sum_{\mathbf{s}\in\phi_1^i} P(\mathbf{r}|\mathbf{s}) \cdot \prod_{l=1,l\neq k}^{N_t\times m} P(c_k)}{\sum_{\mathbf{s}\in\phi_0^i} P(\mathbf{r}|\mathbf{s}) \cdot \prod_{l=1,l\neq k}^{N_t\times m} P(c_k)} \tag{4.8}$$

where ϕ_b^i denotes the symbols whose labels have the value b ("0" or "1") in their i-th position. $P(c_k)$ is denoted as the *a priori* probability of the bit c_k (the k-th bit of the signal $\mathbf{s}$ label).

The *extrinsic* information from the demodulator/demapper is de-interleaved and sent to the BCJR decoder. In fact the de-interleaver between the demodulator and

decoder in the receiver is the counterpart of the interleaver in the transmitter. Therefore the LLR values associated with coded bits move to the original position of bits before being interleaved.

The computation of the *extrinsic* LLR values at the outer decoder, unlike the demodulator/demapper, is only based on *a priori* information obtained from the inner demodulator/demapper. This *extrinsic* LLRs can be computed as

$$L_{e2,b_i} = \underbrace{\ln \frac{P(b_i = 1|\mathbf{L}_{a2}^{b_i})}{P(b_i = 0|\mathbf{L}_{a2}^{b_i})}}_{L_{d2,b_i}} - L_{a2,b_i} \tag{4.9}$$

where $\mathbf{L}_{a2}^{b_i}$ is the vector of the given *a priori* bit LLRs. The associated MAP algorithm has been discussed in detail in Chapter 2. Variables with subscript "2" are associated with outer decoder. In fact the output *extrinsic* LLRs from the inner demodulator after interleaving, are used as the *a priori* information for the outer decoder.

4.3 Sphere Decoder

It is shown that the best approach for computing the *extrinsic* information in equation (4.8) is Maximum Likelihood detection approach. ML promises the optimal performance. In the ML approach, all the constellation points are considered in computing the *extrinsic* information. The major concerns in computing the *extrinsic* LLRs using ML approach, is the complexity. The complexity is growing exponentially with the length of the bit vector $\mathbf{c}$ or in other words the size of multi-dimensional constellation. To compute the *extrinsic* information for each c_i, $2^{N_t \times m}$ calculations should be done, where m is the size of conventional constellation and N_t is the number of dimensions

or transmit antennas. Therefore, ML detection is no feasible. For example in 8 dimensional 16QAM constellation, $2^{32} \approx 2 \times 10^9$ calculation should be performed to compute *extrinsic* information for each bit.

To make its use possible, the ML detection algorithms with reduced complexity have been proposed, such as List Sphere Decoding (LSD) algorithms [31][32][33]. This has been discussed in more details in Chapter 2.

In the proposed receiver in Fig. 4.1, LSD is used as a inner decoder. Therefor, we can rewrite equation (4.8) as follows,

$$L_{e1,c_i} = \ln \frac{\sum_{\mathbf{s}\in\mathcal{L}_1^i} P(\mathbf{r}|\mathbf{s}) \cdot \prod_{l=1,l\neq k}^{N_t\times m} P(c_k)}{\sum_{\mathbf{s}\in\mathcal{L}_0^i} P(\mathbf{r}|\mathbf{s}) \cdot \prod_{l=1,l\neq k}^{N_t\times m} P(c_k)} \tag{4.10}$$

where $\mathcal{L}_b^i$ denotes the symbols in the list whose label have the value b ("0","1") in their i-th position. If there are no entries in $\mathcal{L}$ with $c_i = b$ then radius, d, should be increased. The list size N_c measures how well equation (4.10) approximates equation (4.8). On the other hand the size of the list affects the performance. There is always trade-off between the performance and the list size (complexity). Increasing N_c, results in better performance but higher complexity.

Choosing the radius of the sphere is one of the major concerns in LSD. If the radius d is chosen to be too small, only a few points will be found inside the sphere regardless of how large N_c is. On the other hand if d is chosen to be too large, sphere contains many candidates and this slows down the LSD. Choice of the radius has been discussed in detail in Chapter 2. As it is suggested in [31] during our simulation we find the satisfactory radius by trial and error.

4.4 Simulation Results and Discussion

In this section, simulations are carried out to demonstrate the error performance of the proposed system. Three kinds of proposed constellations/mappings in the table 3.6 are tested. These constellations/mappings are applied to the proposed MIMO transceiver in Fig. 4.1. For simulations, a simple 8 state, rate $\frac{1}{2}$ convolutional code with $g_1 = [1101]$ and $g_2 = [1111]$ is used. Bit-interleaver permutes a 5000-bit block. A MIMO system is considered without any special space-time coding. The MIMO system benefits from spatial multiplexing or in other words uses a V-BLAST method to assure high data rate communications. At the receiver side, the inner detection is based on List Sphere Decoder as discussed in the previous section. Three kinds of channels are assumed.

- AWGN channel where $\mathbf{H} = \mathbf{I}$
- Fast fading channel where the channel randomly changed from one symbol interval to another.
- Slow fading channel where channel keeps constant for a 5000-bit block, and it is randomly changed from one block to another.

The entries of $\mathbf{H}$ (h_{ij}) are assumed to be i.i.d. symmetrical complex Gaussian random variables with zero mean and unit variance. It is assumed that the channel state information or channel matrix $\mathbf{H}$ is perfectly known at the receiver. The radius for LSD is assumed to be fixed. Therefore, the list size may be variable. 2-dimensional QPSK is applied to a 2×2 MIMO system. The comparison between conventional mapping and proposed mapping are illustrated in Figs. 4.2-4.4. It is illustrated that our proposed multi-dimensional constellation/mapping scheme outperforms the

conventional one by 2.7 dB, 3.5 dB and 1.3 dB over AWGN, fast fading and slow fading channels, respectively.

The figures show that at lower SNR, conventional mapping schemes perform slightly better than proposed one. This applies to all three constellations/mappings which are illustrated. It should be noted that the demonstrated SNR in Figs. 4.2 - 4.10, is measured at the transmitter. Also, it should be mentioned that the comparisons between proposed constellations and mappings are made at bit error rate of 10^{-5}.

Figs. 4.5 - 4.7 are depicted simulation results for 2×2 MIMO system using 2-dimensional 8QAM. Simulation results show that our proposed constellation/mapping scheme outperforms the conventional one by 2.5 dB, 2.7 dB and 1.6 dB for AWGN, fast fading and slow fading channels respectively. At the end, 3-dimensional QPSK is applied to a 3×3 MIMO system. Also, Figs. 4.8 - 4.10 show that the proposed 3-dimensional QPSK mapping outperforms the conventional QPSK mapping over 3×3 MIMO system. Simulation results show that, we have 3.3 dB, 2.4 dB and 1.8 dB improvement for AWGN, fast fading and slow fading channels respectively.

In the Chapter 3, it has been mentioned that for the same data rate, 3-dimensional QPSK is preferred to 2-dimensional 8QAM , since the symbol-wise mutual information of 3-dimensional QPSK is higher than 2-dimensional 8QAM, as shown in Fig. 3.10. This is confirmed by the simulation results which the desirable BER can be achieved at lower SNR by applying 3-dimensional QPSK. Also in the table 3.6, it can be noticed that the cost function (δ) for 3-dimensional QPKS is the least between all proposed constellation/mappings. The lower value for δ should result in

better performance which is demonstrated by simulation results of proposed constellations/mappings. Simulations show that significant improvement can be achieved over AWGN, fast fading and slow fading channels. This suggests that equation (3.15) which was obtained for slow fading channel can be used for AWGN and fast fading as well. Moreover, it is demonstrated by simulations that mutual information proposed in the Chapter 3, is a good measure to compare constellations/mappings.

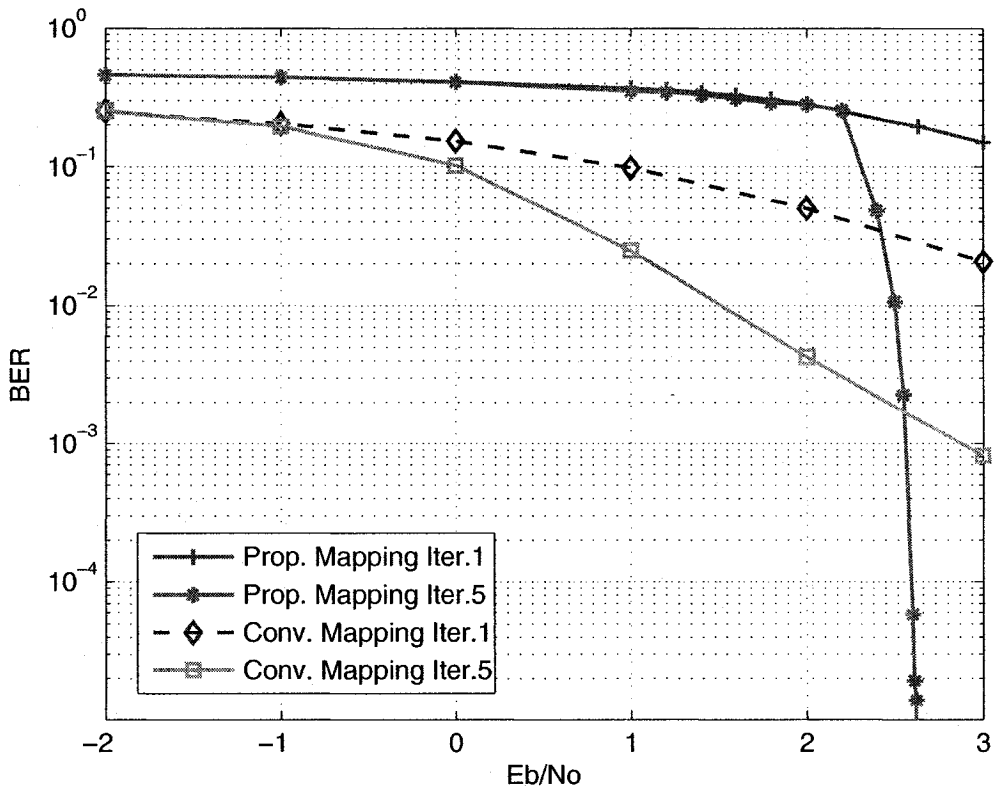

Figure 4.2: BER comparison between the proposed 2-dimesional QPSK and conventional QPSK schemes, using 2×2 MIMO system over AWGN channel

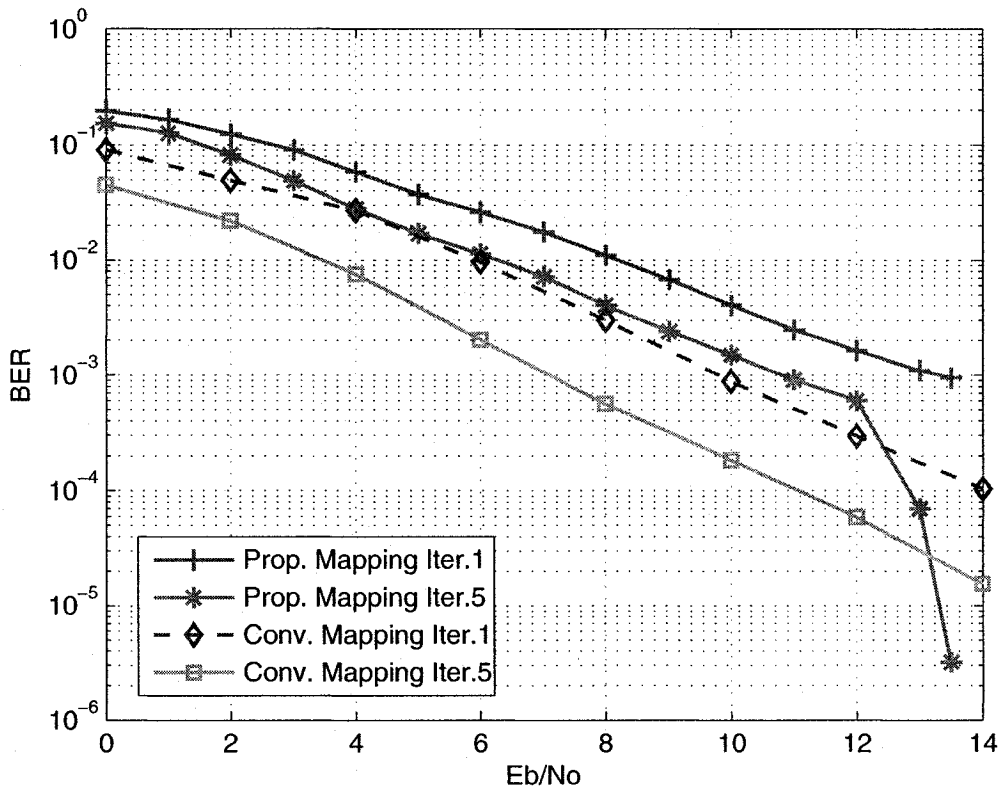

Figure 4.3: BER comparison between the proposed 2-dimesional QPSK and conventional QPSK schemes, using 2×2 MIMO system over slow fading channel

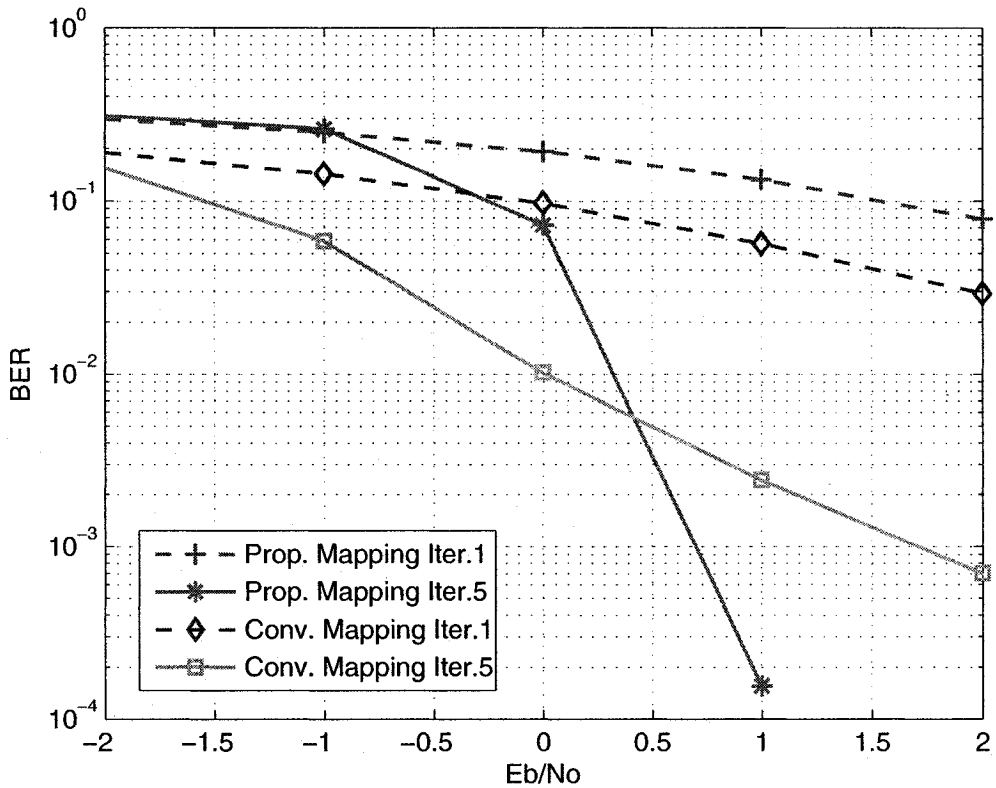

Figure 4.4: BER comparison between the proposed 2-dimesional QPSK and conventional QPSK schemes, using 2×2 MIMO system over fast fading channel

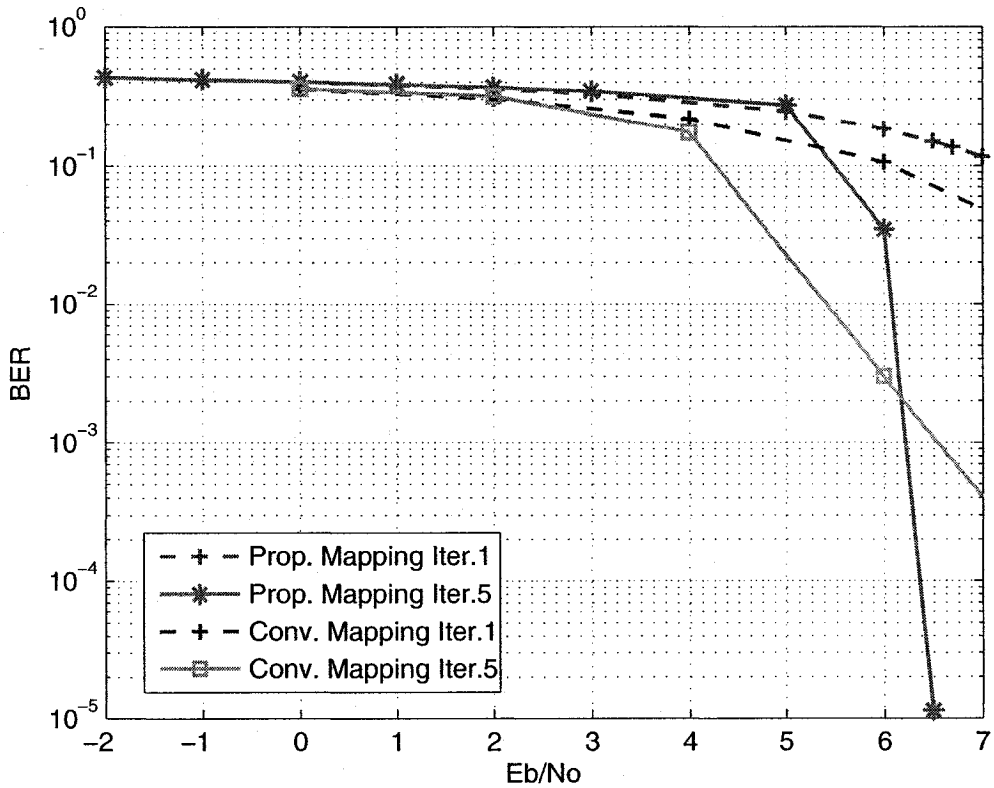

Figure 4.5: BER comparison between the proposed 2-dimesional 8QAM and conventional 8QAM schemes, using 2×2 MIMO system over AWGN channel

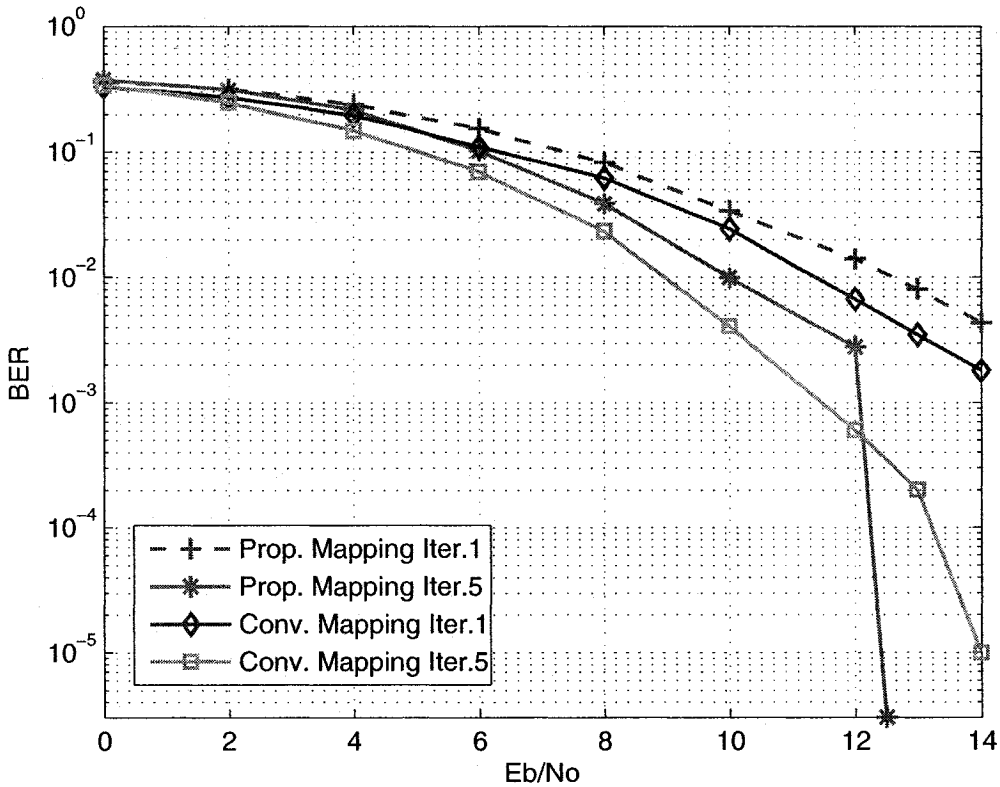

Figure 4.6: BER comparison between the proposed 2-dimesional 8QAM and conventional 8QAM schemes, using 2×2 MIMO system over slow fading channel

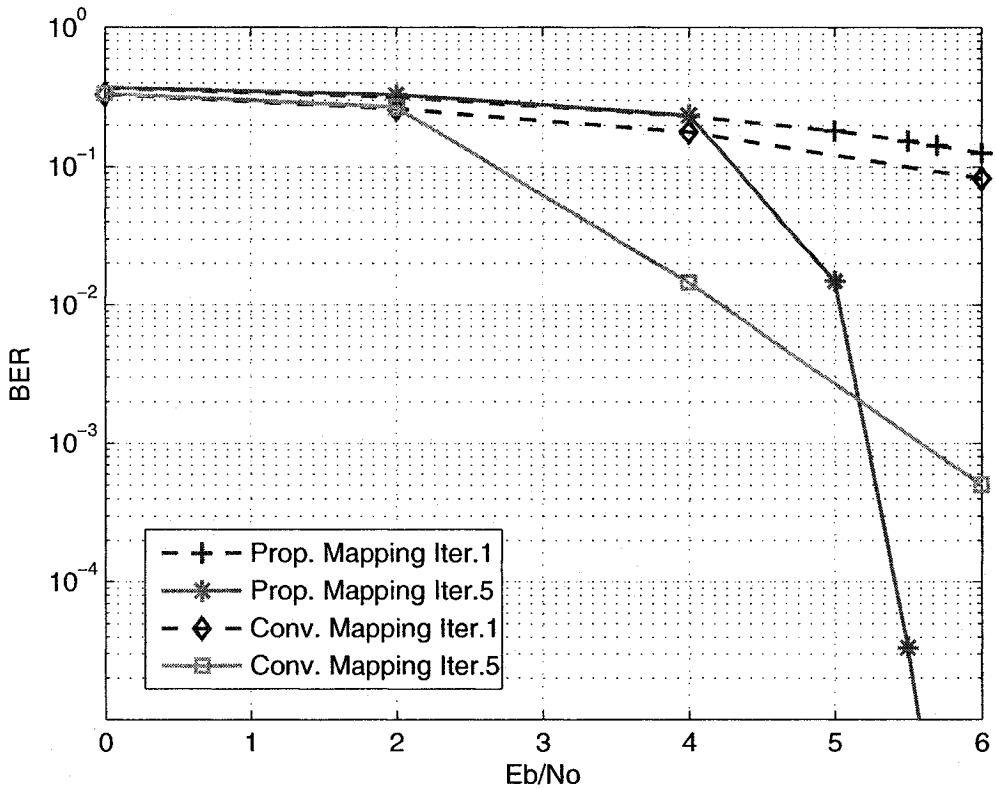

Figure 4.7: BER comparison between the proposed 2-dimesional 8QAM and conventional 8QAM schemes, using 2×2 MIMO system over fast fading channel

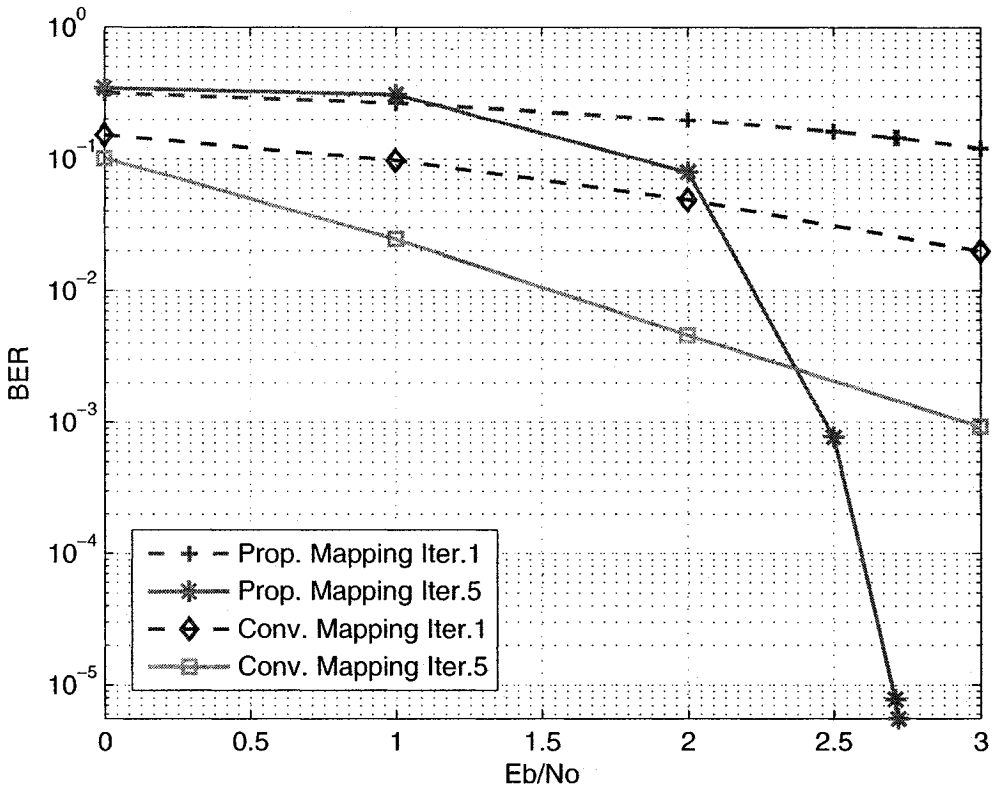

Figure 4.8: BER comparison between the proposed 3-dimesional QPSK and conventional QPSK schemes, using 3×3 MIMO system over AWGN channel

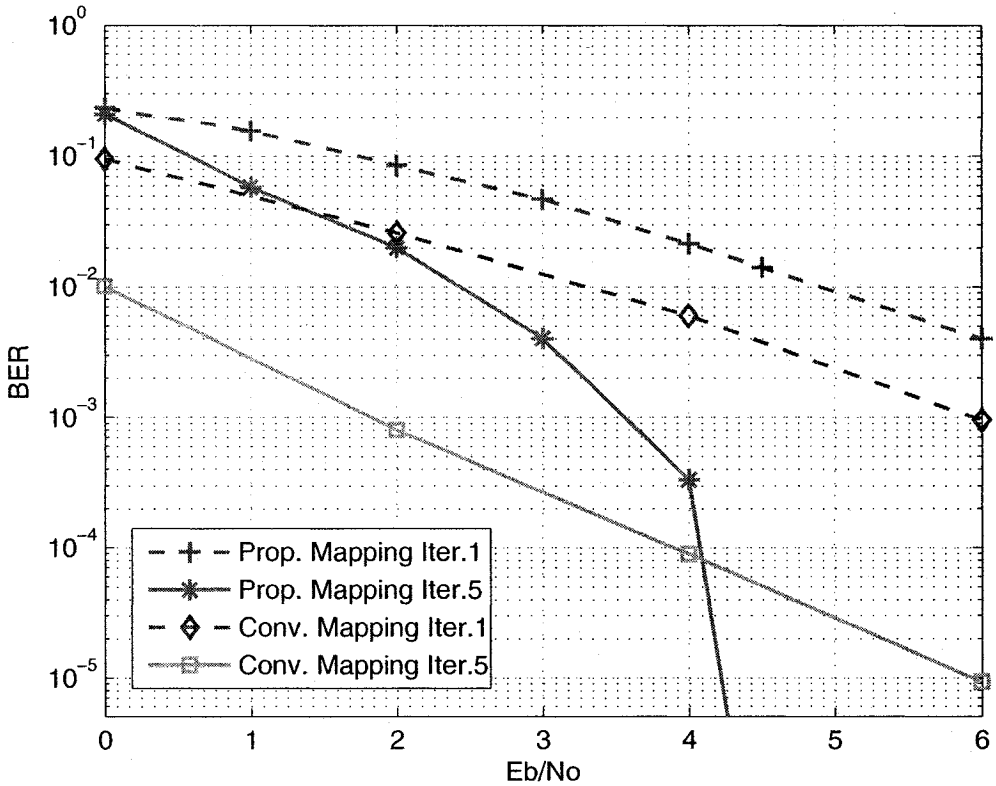

Figure 4.9: BER comparison between the proposed 3-dimesional QPSK and conventional QPSK schemes, using 3×3 MIMO system over slow fading channel

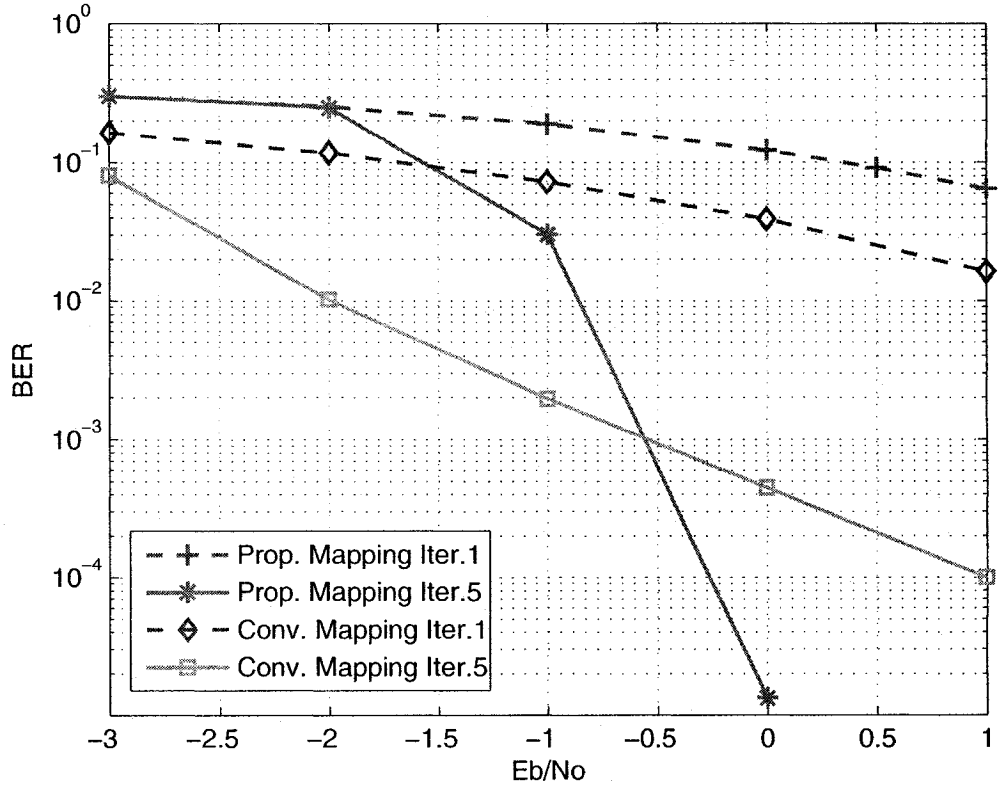

Figure 4.10: BER comparison between the proposed 3-dimesional QPSK and conventional QPSK schemes, using 3×3 MIMO system over fast fading channel

4.5 Summary

The design of the MIMO receiver is crucial, since it should contribute to a good error performance while keeping the complexity reasonable. In this chapter, it was shown that, one of the receiver schemes promising desirable error performance for a MIMO system is iterative decoding. A simple approximation for calculating the *extrinsic* information at the demodulaotr/demapper was also proposed. In the receiver sphere decoder and list sphere decoder was used to decrease complexity.

Moreover, simulation results are illustrated. Three different type of proposed constellations/mappings are applied to the MIMO system. The results show that, proposed constellations/mappings improves the error performance significantly. Also, simulation results show the effect of the cost function value on the error performance. Simulations demonstrated that mutual information is a good measure for comparing different constellations/mapping.

Chapter 5

Summary and Conclusions

In this thesis, the design of constellation/mapping for MIMO-BICM-ID system is studied. Based on minimizing pair-wise error probability, a design criterion is proposed to find the optimal constellation/mapping for MIMO-BICM-ID. To reduce computational complexity of exhaustive search, Binary Switching Algorithm is improved to find the optimal solution. Using the design criterion and employing the Binary Switching Algorithm, some optimal constellations/mappings are found for 2-dimensional and 3-dimensional cases, such as 2-dimensional QPSK, 2-dimensional 8QAM and 3-dimensional QPSK.

A measurement based on mutual information is developed to evaluate the proposed constellations/mappings. The Monte-Carlo numerical results show that the proposed constellations/mappings sacrifice bit-wise mutual information without *a priori* information but gain significantly when *a priori* information feedback is perfect. This suggests that the proposed schemes can achieve better performance if applied to a MIMO-BICM-ID system.

To manage the computational complexity at the receiver, an iterative receiver

based on List Sphere Decoder is employed. The MIMO transceiver with the proposed constellations/mappings can achieve the promised error performance. Simulations were carried out and results show that the proposed mapping schemes outperform the conventional ones significantly at high signal to noise ratio. Although, the design criteria is based on slow fading channel, simulation results also show that proposed mapping schemes perform well over slow as well as fast fading channels.

System simulations were carried out specifically for 2-dimensional QPSK, 2-dimensional 8QAM and 3-dimensional QPSK constellations/mappings. Results show an improvement of 1.3 dB, 1.6 dB and 1.8 dB compared to conventional constellation mappings over slow fading channels, respectively. This improvement increase to 3.5 dB, 2.7 dB and 2.4 dB for fast fading channels.

5.1 Future Work

Some future works of this thesis can be developed as follows:

- Apply the global optimum search instead of locally optimum Binary Switching Algorithm.
- The Design criteria for fast fading channel should be developed.
- Optimal constellations/mappings for other space-time codes should be studied.
- Optimal constellation/mapping for more dimensions and higher order constellations can be investigated.

Bibliography

[1] C. Shannon, "A mathematical theory of communication," *Bell Syst. Tech. J.*, vol. 27, pp. 379–423 (Part one),623–656 (Part two), Oct. 1948. reprinted in book form, University of Illinois Press, Urbana, 1949.

[2] C. Berrou, A. Glavieux, and P. Thitimajshima, "Near shannon limit error-correcting coding and decoding: turbo codes," *Inter. Conf Commun*, pp. 1064–1070, in Proc. 1993.

[3] R. Gallager, *Low Density Parity Check Codes.* MIT Press, Cambridge, Massachusets, 1963.

[4] D. MacKay, "Near shannon limit performance of low density parity check codes," *Electronics Letters*, vol. 32, pp. 1645–1646, August 1966.

[5] I. E. Telatar, "Capacity of multi-antenna gaussian channels," *European Transactions on Telecommunications*, vol. 10, pp. 585–595, Nov/Dec 1999.

[6] G. Foschini and M. Gans, "On limits of wireless communications in a fading environment when using multiple antennas," *Wireless Personal Communications*, vol. 6, pp. 311–335, 1998.

[7] J. Massey, "Coding and modulation in digital communications," in Proc. of International Zurich Seminar on digital communications, March 1974.

[8] G. Ungerboeck, "Channel coding with multilevel/phase signals," *IEEE Transactions on Information Theory*, vol. IT-28, pp. 55–67, January 1982.

[9] D. Divsalar and M. Simon, "The design of trellis coded mpsk for fading channels: performance criteria," *IEEE Transactions on Communications*, vol. 36, pp. 1004 – 1012, September 1988.

[10] B. Jelicic and S. Roy, "Design of trellis coded QAM for flat fading and AWGN channels," *IEEE Transactions on Vehicular Technology*, vol. 44, pp. 192 – 201, Feb 1995.

[11] E. Zehavi, "8-PSK trellis codes for a rayleigh channel," *IEEE Transactions on Communications*, vol. 40, pp. 873–884, May 1992.

[12] K. Boulle and J. Belfiore, "Modulation schemes designed for the rayleigh channel," *IEEE International Symposium on Information Theory*, pp. 342 – 342, Jan. 1993.

[13] G. Caire, G. Taricco, and E. Biglieri, "Bit-interleaved coded modulation," *IEEE Transactions on Information Theory*, vol. 44, pp. 927–946, May 1998.

[14] X. Li and J. Ritcey, "Bit-interleaved coded modulation with iterative decoding," *IEEE Communications Letters*, vol. 1, November 1997.

[15] X. Li, A. Chindapol, and J.A. Ritcey, "Bit-interleaved coded modulation with iterative decoding and 8PSK signaling," *IEEE Transaction on communications*, vol. 50, August 2002.

[16] P. Robertson, "Bandwidth-efficient turbo trellis-coded modulation using punctured component codes," *IEEE Journal on Selected areas in communications*, vol. 16, February 1998.

[17] S. M. Alamouti, "A simple transmit diversity technique for wireless communications," *IEEE journal on select areas in cummunications*, vol. 16, October 1998.

[18] V. Tarokh, N. Seshadri, and A. Calderbank, "Space-time codes for high data rate wireless communications: Performance criterion and code construction," *IEEE Transactions on Information Theory*, vol. 44, pp. 744–765, March 1998.

[19] V. Tarokh, H. Jafarkhani, and A.R. Calderbank, "Space-time block code from orthogonal designs," *IEEE Transactions on Information Theory*, vol. 45, pp. 1456–1467, July 1999.

[20] D. Gesbert, M. Shafi, Da–shan Shiu, P.J. Smith, and A. Naguib, "From theory to practice: an overview of mimo space-time coded wireless systems," *IEEE Journal on Selected Areas in Communications*, vol. 21, pp. 281–302, April 2003.

[21] P.W. Wolniansky, G.J. Foschini, G.D. Golden, and R.A. Valenzuela, "V-blast: An architecture for realizing very high data rates over the rich-scattering wireless channel," *IEEE Proceedings of ISSSE-98*, Sept 1998.

[22] G.J. Foschini, G.D. Golden, R.A. Valenzuela, and P.W. Wolniansky, "Simplified processing for high spectral efficiency wireless communication employing multi-element arrays," *IEEE Journal on Selected Areas in Communications*, vol. 17, pp. 1841–1852, Nov 1999.

[23] G.D. Golden, G.J. Foschini, R.A. Valenzuela, and P.W. Wolniansky, "Detection algorithm and initial laboratory results using the V-BLAST space-time communication architecture," *Electornics Letters*, vol. 35, pp. 14–16, January 1999.

[24] L. Zhang and D. Tse, "Diversity and mutiplexing: A fundamental tradeoff in multiple antenna channels," *IEEE Transaction on Information Theory*, vol. 49, pp. 1073–1096, May 2003.

[25] S.H. Müller-Weinfurtner, "Coding approaches for multiple antenna transmission in fast fading and ofdm," *IEEE Transaction on Signal Processing*, vol. 50, pp. 2442–2450, Oct 2002.

[26] J.J. Boutros, F. Boixadera, and C. Lamy, "Bit-interleaved coded modulations for multiple-input multiple-output channels," *IEEE Sixth International Symposium on Spread Spectrum Techniques and Applications*, vol. 1, pp. 123–126, 6-8 Sept. 2000.

[27] N. H. Tran and H. H. Nguyen, "Signal mappings of 8-ary constellations for bit interleaved coded modulation with iterative decoding," *IEEE Transactions on Broadcasting*, vol. 52, March 2006.

[28] N. H. Tran and H. H. Nguyen, "Signal mappings of 8-ary constellations for bicm-id over a rayleigh fading channel," in *Canadian Conference on Electrical and Computer Engineering*, vol. 3, pp. 1809–1813, May 2004.

[29] F. Schreckenbach, N. Gortz, J. Hagenauer, and G. Bauch, "Optimized symbol mappings for bit-interleaved coded modulation with iterative decoding," in *IEEE*

Global Telecommunications Conference ,GLOBECOM '03, vol. 6, pp. 3316–3320, Dec 2003.

[30] K. Zeger and A. Gersho, "Pseudo-gray coding," *IEEE Transactions on Communications*, vol. 38, pp. 2147–2158, December 1990.

[31] B. M. Hochwald and S. ten Brink, "Achieving near-capacity on a multiple-antenna chanel," *IEEE Transactions on Communications*, vol. 51, pp. 389–399, March 2003.

[32] M. Pohst, "On the computation of lattice vectors of minimal length, successive minima and reduced basis with applications," *in Proc. ACM SIGSAM*, vol. 15, 1981.

[33] B. Hassibi and H. Vikalo, "On the sphere-decoding algorithm i. expected complexity," *IEEE Transactions on Signal Processing*, vol. 53, pp. 2806–2818, August 2005.

[34] S. Lin and D. Costello, *Error Control Coding.* Prentice-Hall, Inc. Englewood Cliffs, New Jersey 07632, 1983.

[35] X. Li and J.A. Ritcey, "Bit-interleaved coded modulation with iterative decoding," *IEEE Communications Letters*, vol. 1, pp. 169–171, Nov. 1997.

[36] J. Proakis, *Digital Communications.* Singapore: McGraw-Hill, 1989.

[37] D. Cui and A. M. Haimovich, "Design and performance of turbo space-time coded modulation," *IEEE GLOBECOM00*, vol. 3, pp. 1627–1631, Nov. 2000.

[38] D. Tujkovic, "Recursive space-time trellis codes for turbo coded modulation," *Proc. of GlobeCom 2000*, San Francisco, 2000.

[39] Y. Liu and M. Fitz, "space-time turbo codes," *13th Annual Allerton Conf. on Commun. Control and Computing*, September 1999.

[40] G. J. Foschini, "Layered space-time architecture for wireless communication in fading environment when using multiple antennas," *Bell System Tech. Journal*, vol. 1, no. 2, pp. 41–59, 1996.

[41] S. Hayki, *Communication Systems.* John Wiley & Sons Inc., 2001.

[42] N. Tran and H. Nguyen, "Multi-dimensional mappings of m-ary constellations for bicm-id systems," in *Canadian Conference on Electrical and Computer Engineering*, pp. 135–138, May 2005.

[43] F. Simoens, H. Wymeersch, H. Bruneel, and M. Moeneclaey, "Multidimensional mapping for bit-interleaved coded modulation with BPSK/QPSK signaling," *IEEE ,Communications Letters*, vol. 9, pp. 453–455, May 2005.

[44] J. Boutros, N. Gresset, and L. Brunel , "Turbo coding and decoding for multiple antenna channels," *International Sympsium on Turbo Codes and Related Topics*, September 2003. Brest.

[45] J. Hagenauer, "The exit chart- introduction to extrinsic information transfer in iterative processing," in *EUSIPCO*, (Vienna, Asutria), September 2004.

[46] S. ten Brink, "Designing iterative decoding schemes with the extrinsic information transfer chart," *AEÜ International Journal of Electronics and communications*, vol. 54, pp. 389–398, November 2000.

[47] S. ten Brink, "Convergence behavior of iteratively decoded parallel concatenated codes," *IEEE Transactions on Communications*, vol. 49, pp. 1727–1737, October 2001.

[48] S. ten Brink, J. Speidel, and Ran-Hong Yan, "Iterative demapping and decoding for multilevel modulation," *IEEE Global Telecommunications Conference, 1998. GLOBECOM 98. The Bridge to Global Integration.*, vol. 1, pp. 579–584, November 1998.

[49] S. ten Brink, "Convergence of iterative decoding," *Electronics Letters*, vol. 35, pp. 1117–1119, June 1999.

[50] L. Bahl, J. Cocke, F. Jelinek, and J. Raviv, "Optimal decoding of linear codes for minimizing symbol error rate," *IEEE Transactions on Information Theory*, vol. 20, pp. 284–287, March 1974.